University of Catania

International PhD in Translational Biomedicine XXVIII cycle

PhD COORDINATOR PROF. DANIELE FILIPPO CONDORELLI

ALESSANDRO SINOPOLI

Molecular mechanisms of Aβ recognition and neuroprotection by the glycoconjugate β-sheet-breaker peptide Ac-LPFFD-Th.

PhD THESIS

PhD Supervisor :

Prof. Daniele F. Condorelli

PhD Co-Supervisor:

Dott. Giuseppe Pappalardo

2013 – 2015

TABLE OF CONTENTS

Abstract

Inhibition of amyloid formation may represent a promising therapeutic approach for the treatment of neurodegenerative diseases. To this regard, peptide-based inhibitors of Aβ aggregation have been widely investigated with a particular emphasis to those derived from original amyloid sequences.

The experimental work described in the present PhD Thesis aims at outlining the molecular mechanisms underlying the antifibrillogenic and neuroprotective action exhibited by a new class of trehalose conjugated pentapeptides. Trehalose (Th), a non-reducing disaccharide of α-(D)glucose, has been demonstrated to be effective in preventing the aggregation of several proteins. We figured out that the development of hybrid compounds may provide new molecules with improved properties that might sinergically increase the potency of their single moieties.

Since it has been demonstrated that Aβ oligomers are the toxic species, it becomes a priority to counteract the Aβ self-assembly because of its doubly dangerous effect associated with oligomers generation and removal of the neurotrophic monomeric form of Aβ1-42 peptide.

Starting from the well-known neuroprotective action of the LPFFD peptide, (C. Soto, *Nat Med*. 1998) we investigated whether the Ac-LPFFD-Th peptide would act as an "Aβ *monomer-stabilizer*" thus exerting a neuroprotective activity. In support of this hypothesis, time-resolved proteolysis and ESI-MS experiments, performed during my PhD experimental work, showed a direct interaction between these β-breaker peptides and Aβ monomers.

In this work, the C-terminal trehalose conjugated Ac-LPFFD-Th derivative ability to recognize and bind low molecular weight aggregated forms of Aβ has been investigated by means of different biophysical techniques, including Th-T fluorescence, DLS, ESI-MS and NMR. Furthermore, biological assays on murine cortical primary neuronal cultures were performed in order to clarify and further characterize the mechanism of cytoprotection exhibited by the Ac-LPFFD-Th.

In this PhD thesis, we demonstrated that Ac-LPFFD-Th modifies the aggregation features of Aβ and protects neurons from Aβ oligomers' toxic insult.

Introduction

1.1 PROTEIN FOLDING, MISFOLDING and AMYLOIDOSIS.

Proteins after their synthesis in the cell, must be converted into tightly folded compact structures in order to function. Many of these structures are astonishingly intricate, the fact that folding is usually exceptionally efficient is an outstanding evidence of the power of evolutionary biology. Given that there are 20 different naturally occurring amino acids, the total possible number of different proteins with the average size of those in our bodies is enormous. The properties of the natural proteins are not typical of random sequences, but have been selected through evolutionary pressure in order to have specific characteristics of which the capacity to fold to unique structures and therefore to generate enormous selectivity, in addition to the diversity in their functions. (1)

How proteins find their distinctive native folded states from the information enclosed in their sequences is a question at the heart of molecular biology.(1)

The mechanism by which also the smaller and easier proteins fold to unique structures has been defined in detail. There are strong evidences that the native state of a protein corresponds, except in very exceptional circumstances, to the most stable structure under physiological conditions.

However, the total number of possible conformations of a protein is so great that it would take an enormous amount of time to find this particular structure throughout a systematic search of all the conformational space.(2,3)

Now it is clear that the folding of a protein does not involve a succession of compulsory steps between well-defined partially folded states, but rather a stochastic search of the many conformations accessible to a polypeptide chain. In principle, the inherent fluctuations in the conformation of an unfolded polypeptide chain allow even residues at very different positions in the amino acid sequence to come in contact with the others. Since the correct (native-like) interactions between the different residues are generally more stable than the incorrect (non-native) ones, such a search mechanism is, in theory, able to find the lowest energy structure possible between all the different conformations. (1-4)

It is clear that this process is particularly efficient for those sequences that have been selected during evolution to fold into globular structures, and in fact, only a very little number of all possible conformations needs be sampled during the search process. This stochastic description of protein folding introduces the concept of an "energy landscape". (1) This describes the free energy of the polypeptide chain as a function of its conformational properties. In order to enable a protein to fold correctly and efficiently, the landscape required has been associated to a funnel because the conformational space easily accessible to the polypeptide chain becomes more and more restricted as the native state is closer (figure 1). (1-4)

The elevated degree of disorder of the polypeptide chain is reduced as the folding progresses because there is a gain in enthalpy related with all the stable native-like interactions that are created. This gain in enthalpy can counterbalance the decreasing in entropy of the polypeptide chain as the structure becomes more ordered. (5*a*)

Even though the details of the way in which the different proteins can fold may appear to differ considerably, in terms of the rates of folding and the type of species populated during the folding process, the fundamental features of this general mechanism can be considered to be universal. (1,5)

Hence globular proteins mainly fold by minimizing the non-polar surface that is exposed to water, while at the same time forming hydrogen interactions for buried backbone groups, typically in the form of secondary structures such as α-helices, β-sheets, and tight turns. (5*b*)

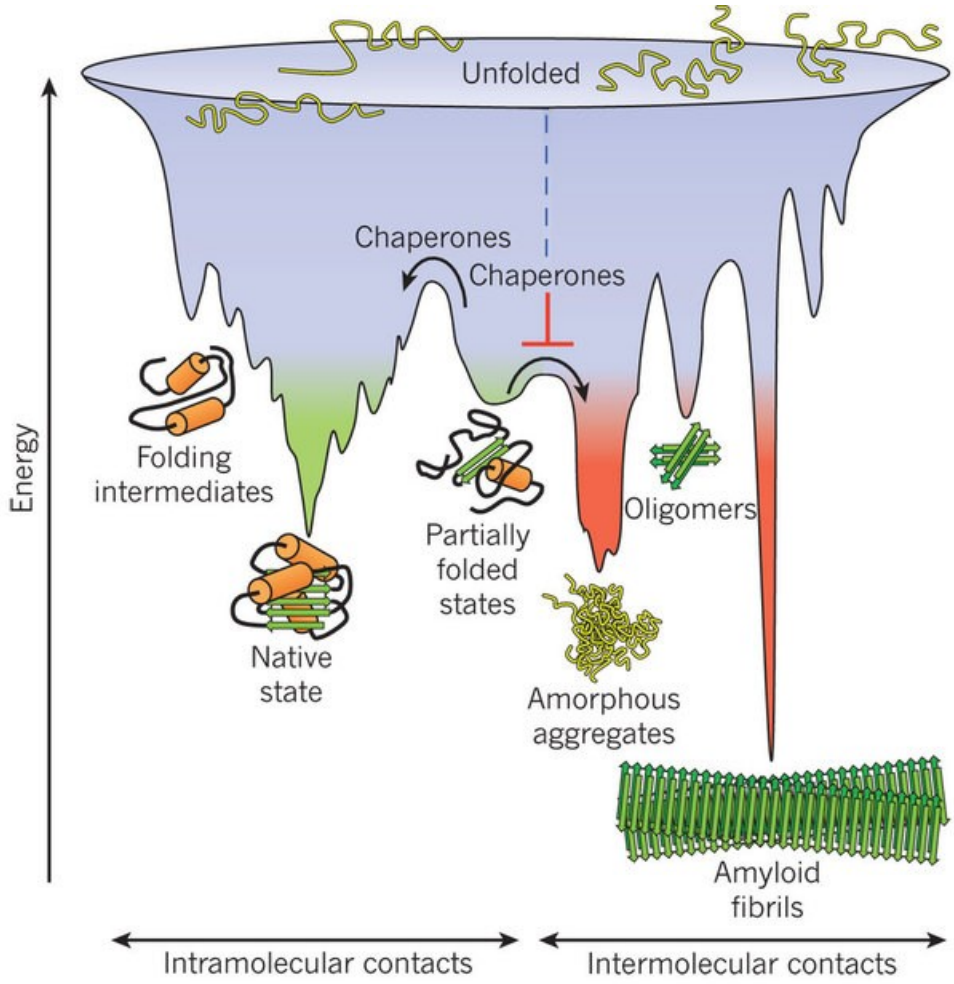

Figure 1. Protein folding and proteostasis. (Nature 2011, 475, 324–332).

The folding of some proteins in vivo appears to be co-translational, it means that the folding begins when the growing chain is still being synthesized on the ribosome (6). Because of the complexity of the folding process, misfolding is an inherent feature of it for all proteins, particularly under unfavorable environment conditions.

Misfolding can roughly be defined as reaching a state that has a significant proportion of nonnative interactions between residues and whose properties differ considerably from those of a similar state having native-like interactions. The cellular levels of many chaperones are, as a matter of fact, significantly increased during cellular stress, from that their common designation as heat-shock proteins (Hsps). Some of these molecular chaperones act to capture misfolded proteins, or even some types of aggregates, and so giving them another opportunity to fold correctly. (7)

One of the better known characteristic features of many of the misfolding diseases is that they often result in to the deposition of proteins in form of amyloid fibrils, stable, ordered, filamentous protein aggregates. A significant number of human diseases, including neurodegenerative diseases such as Alzheimer's disease, Parkinson's diseases, prion diseases, Amyotrophic lateral sclerosis (ALS), Type 2 diabetes mellitus and several other pathological conditions share a common feature.

In each of these pathologies, protein or peptide changes from their natural soluble state into insoluble fibrils, which aggregate and accumulate in a variety of tissues and organs. Although approximately 20 different proteins are known to be involved in the amyloidoses, they are generally unrelated in terms of sequence or structure. Despite these differences in sequence and structure, the fibrils formed from these different peptides or proteins in diverse pathologies share many common properties. Those are a core cross-β-sheet structure in which continuous β-sheets are formed with β-strands running perpendicular to the long axis of the fibrils. (8) All fibrils have similar morphologies, being twisted, rope-like structures, reflecting a filamentous substructure. (9)

Disease	Protein	Site of folding
Hypercholesterolaemia	Low-density lipoprotein receptor	ER
Huntington's disease	Huntingtin	Cytosol
Cystic fibrosis	Cystic fibrosis *trans*-membrane regulator	ER
Tay–Sachs disease	Hexosaminidase	ER
Alzheimer's Disease	Amyloid β peptide/ Tau	ER
Parkinson's disease	α-Synuclein	Cytosol
Creutzfeldt–Jakob disease	Prion protein	ER
Familial amyloidoses	Transthyretin/Lysozyme	ER
Cataracts	Crystallins	Cytosol
Diabetes	Amylin	Cytosol

Table 1. Protein misfolding in conformational diseases

1.2 ALZHEIMER'S DISEASE and AMYLOID-β.

Alzheimer disease (AD) is the most prevalent neurodegenerative disease affecting more than 35 million people worldwide. (10)

Despite considerable research, there is no cure for this pathology yet and available treatments are only symptomatic.

AD is characterized by progressive loss of memory, declining cognitive function, decreased physical function and ultimately death. It represents one of the main public health challenge of growing significance among the aged population. (11)

The hallmarks of AD are the amyloid plaques, protein aggregates deposited in the brain, and neurofibrillary tangles, intraneuronal bundles of paired abnormally phosphorylated tau proteins.

The generation and aggregation of Aβ activate a complex pathologic cascade leading to neuronal dysfunction, inflammation and neuronal loss. This cascade plays a central role in pathogenesis and is commonly referred to as the amyloid cascade hypothesis. (12) The amyloid hypothesis states that the 39–43 amino acid amyloid-β-peptides (Aβ), the main constituent of amyloid plaques, are responsible for the initiation of a neurotoxic cascade that ultimately leads to neuronal death and dementia. (12)

The Aβ peptides are generated by the cleavage of amyloid precursor protein (APP), a type I integral transmembrane protein. The processing of APP takes place via amyloidogenic and non-amyloidogenic pathway (figure 2).

The normal non-amyloidogenic pathway cleaves APP at amino acid positions 16 and 17, generating a secreted APP derivative sAPPa and a shorter C-terminal fragment (CTF) of 83 amino acids (C83). C83 is subsequently cleaved by γ-secretase to form a non-toxic 3 kDa peptide (p3). Although Aβ is produced normally in the CNS, these α- and β-pathways may compete for APP substrate. APP is believed to be cleaved preferentially through this pathway in normal brain, with the balance shifting to the amyloidogenic pathway in AD. In the amyloidogenic pathway, cleavage occurs within the ecto-domain of APP mediated by β-site APP cleaving enzyme β-secretase (Bace-1, memapsin-2, ASP-2). Cleavage occurs at methionine (position 671) and aspartic acid (position 672) to generate a secreted amino terminal APP derivative (sAPPβ) and a membrane-inserted CTF (β-CTF) of 99 amino acids in length (C99).

C99 is further cleaved by the intramembranous γ-secretase cleavage at 711–713 to the catalytic subunit presenilin, to facilitate cleavage within the hydrophobic lipid bilayer. This cleavage generates the Aβ at the C-terminus and liberates the Aβ peptide into the extracellular space. (13)

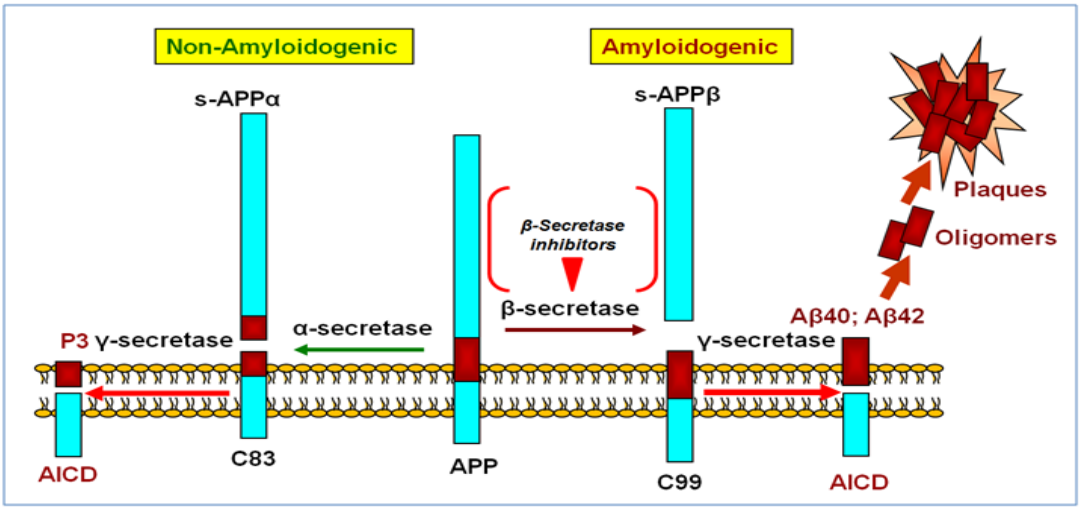

Figure 2. Amyloid cascade hypothesis (C. Zhang. *Discovery Medicine,* 2012, 14, 189-197)

Due to its biophysical properties, under certain condition Aβ 1-40/42 may self-aggregate into different forms, from 4 kDa monomers to dimers, trimers, tetramers, dodecamers, higher-order oligomers, protofibrils, and finally mature fibrils. Fibrils are responsible for the formation of plaques in AD brains. Several environmental factors, such us pH, metal ions and oxidative stress may contribute to the destabilization of the native random coil Aß conformation leading it to aggregation. Although there are accumulating evidence that soluble oligomers are the most cytotoxic form of Aβ, it is still unclear which size and morphology of the aggregates exert neurotoxicity; it has been observed that there is a decrease in toxicity when $A\beta_{1\text{-}42}$ oligomers grow in size. (14)

A new pathological role for Aβ in AD has been observed due to its essential function in the synapse. It is supposed that Aβ may play a variety of physiological roles.

Proposed functions of Aβ include neural metabolism control of synaptic activity, memory consolidation, trophic and neuronal survival, cholesterol transport.

As a matter of fact it seems that the protective or negative effects of Aβ depends by its relative concentration as well as the age-related changes in the cellular environment. (15)

In the human brain, Aβ is generally found in the interstitial fluid; considering its significant affinity for metal ions, due to the presence of three His in the N-terminal part, Aβ could have a function in removing unbound iron, copper and zinc from the extracellular space, stimulating an inflammatory response in microglia which would in turn promote rapid phagocytosis of the peptide.

Therefore, the binding Aβ to metal ions could be a mechanism to remove potentially hazardous metal ions from the extracellular space and to facilitate their clearance from the brain. (16) Moreover it was demonstrated that monomeric Aβ1–40 interacting with metal ions quenches the transition metal-mediated oxygen radical generation, e exerting a neuroprotective effect on neurons. Noteworthy the oligomeric forms of Aβ loose this protective property. These results point out new ideas about the dualistic biological function of Aβ. As a monomer it behaves as an antioxidant molecule, preventing the generation of oxygen radicals, while oligomeric or aggregated forms not only lose antioxidant activity but also contribute to the generation of ROS. (17)

Recent work has shown that monomeric Aβ1–42 in the 30-100 nM concentration range is able to activate the survival pathway in cultures of rat cortical neurons in condition of trophic deprivation, it also protects neurons against NMDA-mediated excitotoxicity cell-death. This effect was mediated by the activation of IGF1/Insulin receptor which trigger the PI-3-K (phosphatidylinositol-3-kinase) pathway. Furthermore, it was shown an increased expression of the antiapoptotic protein Bcl-2.

On the other hand, the Aβ peptide carrying the mutation (E22G) the so-called “Arctic mutation” which is characterized by a rapid aggregation kinetic, it shows a complete loss of neuroprotective activity.(18)

Inflammation is a very important marker in AD as it has been shown in recent works which suggest that, once inflammation is initiated in response to neurodegeneration this may actively contribute to disease progression (figure 3).

Numerous neuroinflammatory mediators are involved such as: cytokines, chemokines, complement activators and inhibitors, radical oxygen species (ROS) and inflammatory enzymes, including the cyclooxygenase-2 (COX-2) as well as the inducible nitric oxide synthase (iNOS). (19,20)

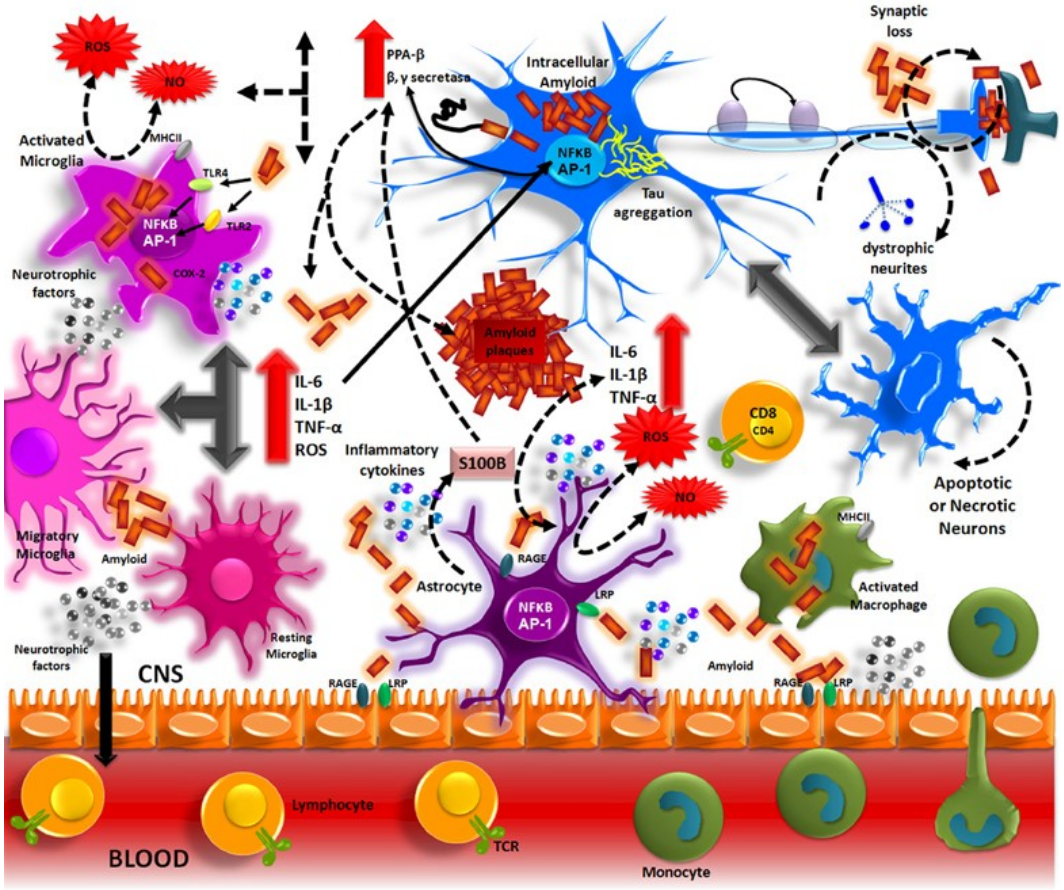

Figure 3. Inflammatory process in Alzheimer's Disease (M.A. Meraz-Ríos et all. *Front. Integr. Neurosci.,* 2013)

It has been shown that Aβ can specifically bind to phospholipid bilayers with relatively high affinity suggesting that the cell membrane of neurons may be a primary target of Aβ. Numerous membrane models including lipid monolayers, bilayers and liposomes, have been used to examine the interactions between Ab and membrane surfaces. The interactions between lipid bilayers and Aβ have been studied using a variety of biophysical techniques, including fluorescence spectroscopy, DSC, CD and NMR. (21*a*)

It was suggested that the head-group charge of the phospholipids contributes to the association between Aβ and the membrane via electrostatic interactions.

Aβ has been reported to form ionic pores, directly leading to cell death or starting the apoptotic signaling interfering with the regulation of calcium homeostasis. (21*b*,22)

Aβ is also able to alter the physicochemical properties of neuronal membranes (e.g. membrane fluidity), and so inducing membrane destabilization and permeabilization. Both membrane-Aβ interactions and toxicity seem to be modulated by the lipid composition, particularly cholesterol and ganglioside, which are speculated to be the major components in the lipid-raft domains of the plasma membrane. It has been reported that cholesterol enhances the binding of Aβ to a lipid bilayer and facilitates Aβ aggregation. (23*a*) However, the role of cholesterol in AD remains controversial. Inconsistent data and conclusions reported in the literature make it difficult to determine the exact mechanism underlying the membrane-associated toxicity of Aβ. The lack of a clear and detailed description of Aβ-membrane interactions hinders a complete understanding of Aβ toxicity in AD pathogenesis. (23*b*)

Several works indicate that the Aβ forms which interact with the membranes, leading to the formation of pores, are associated to microscopic structures similar to very small fibrils, but not to unstructured forms of Aβ. These results strongly suggest that Aβ oligomers are directly involved in destabilization and/or perforations of the synaptic membranes. (24)

It has been demonstrated that amyloid fibrils, usually considered as highly stable and biologically inert structures, can be destabilized and easily reverted to soluble and highly toxic Aβ smaller aggregates by the biological lipids present in the brain. (25) This suggests that part of the critical balance between toxic and inert Aβ pools could be determined by the relative amounts of lipids in the direct environment of the plaques. Surprisingly, the identified toxic species share many properties with the oligomeric aggregates in terms of biophysical and cell biological behavior. Different biophysical assays show how these structures are quite heterogeneous in nature, and the size distribution of these oligomeric aggregates ranges from 80 to 500 kDa. Lipids are apparently promoting the equilibrium toward the protofibrillar pools, inducing toxicity of the amyloid mixture.

Furthermore there is an evidence that membrane composition and properties play a critical role in Aβ cytotoxicity associated with its conformational changes and aggregation into oligomers and fibrils. (25)

A wide range of AD synapto-toxic Aβ oligomeric sizes have been identified. How oligomer size precisely is related to the disease process has not been clarified and recent work shows that the wide range of Aβ oligomers may have a specific conformation in common.

These findings suggest that Aβ oligomer size may not be the only AD-inducing factor but both oligomer size and structural conformation act as toxic parameters in AD progress. Previous studies targeting the Aβ toxic species in AD have usually highlighted only one of these aspects. Instead it is necessary a multi disciplinary approach where oligomer size and structural characteristics should be taken into consideration together. (26) In the typical cross-β-structure, hydrogen bonds are oriented parallel to the fibril axis, with the β -strands running perpendicular to the fibril's axis, usually from 2 to 9 protofilaments form fibrils. However, the amyloid formation is a very complex process, biophysical studies performed in presence of component of the extracellular matrix such as glycosaminoglycans and well-defined model membranes have shown that a variety of amyloidogenic peptides and protein readily adopt helical structures when interacting with surfaces. These generated helical intermediates generated appear to play an important role in amyloid growth in which helix-mediated association will lead to a high local concentration of an aggregation prone sequence, and so favoring intermolecular β-sheet formation. (27)

It has been reported that monomeric Aβ1–40 shows a β-hairpin comprising residues 17–36, in which the 17-23 and the 30-36 fragments make intramolecular backbone hydrogen bonds to form the two central strands of the β-sheet. Both faces of the β-hairpin are predominantly apolar, for this reason they are buried inside a large hydrophobic tunnel-like cavity with the ''interior'' face of the hairpin containing Leu-17, Phe-19, Ile-32, Leu-34, and Val-36 side chains docked into the cleft to form a large intermolecular hydrophobic core. It can be speculated that the β-hairpin constitutes an intermediate conformation on the formation of amyloid fibrils. Therefore oligomers might form by hydrophobic interactions of β-hairpins and remain soluble as a consequence of the hydrophilic surface due to the hydrogen bond capacity of the exposed peptide backbones.

Fibril seeds could subsequently be generated by a concerted conformational transition toward intermolecular β-sheets. (28)

Amyloid aggregation is described by a sigmoidal curve and is considered to be a nucleation–polymerization reaction where the monomer addition steps are assumed to be thermodynamically unfavorable until a critical nucleus is formed.

However, aggregation is a thermodynamically favorable process during the polymerization stage. The critical nucleus is defined as the least thermodynamically stable species in solution, which is the oligomer of minimal size capable of initiating further growth. The nucleus can also be defined as the aggregate size after which the association rate exceeds the dissociation rate for the first time. In addition to the homogeneous nucleation, heterogeneous nucleation (or seeding) can also take place on the surface of existing polymers. Furthermore, aggregation can be further accelerated by the fragmentation of existing aggregates. For some proteins with specific distributions of polar and hydrophobic residues (e.g. for Aβ1–40 peptide), fibrillation can start only above a certain critical micelle concentration at which the peptide micelles are formed.

The formation of these micelles represents a crucial step, as fibrils nucleate inside them and then grow by irreversible binding of monomers to fibril ends.

In addition to the amyloid fibrils discussed above, proteins can self-assemble to form several other types of aggregate such as amorphous aggregates. Amorphous aggregates are typically formed faster than fibrils. There is no special conformational prerequisite for amorphous aggregation to occur, and many destabilized and partially unfolded proteins precipitate out of solution in a form of amorphous aggregate. On the other hand, fibrillation requires special conditions that promote the formation of the specific amyloidogenic conformations. Therefore the conformations of monomers at different aggregation stages are not identical, and a given protein can self-assemble into various aggregated forms, depending on the peculiarities of its environment. Aβ oligomers have shown a wide range molecular mass distribution (from <10 to >100 kDa) in the AD brain (figure 4). *In vitro* studies have revealed that Aβ dimers were three times more toxic than monomers, in addition to Aβ tetramers that were 13 times more toxic, as well as the SDS-stable Aβ nonamers and dodecamers which were shown to induce a significant fall-off in the spatial memory performance and can be associated with deleterious effects on cognition. (29)

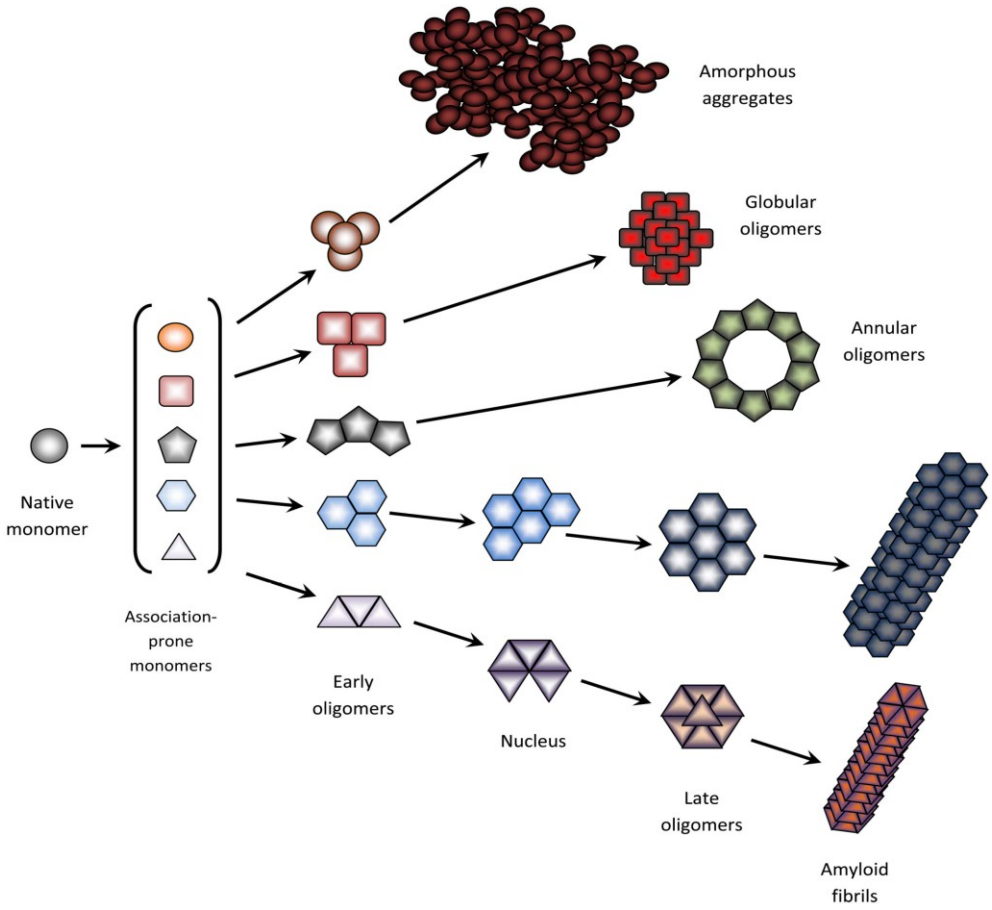

Figure 4**.** Different morphologies of Aβ aggregates *(FEBS J.* 2010, 277, 2940–2953)

The structure of Aβ fibrils is determined by constraints due to the monomer's conformation, interestingly, fibril structure formation is determinate also by the kinetic of the process rather than the thermodynamically lowest energy state.

It was hypothesized that the predominant fibrillar structure would be the one with the fastest kinetics of formation even though more thermodynamically stable states might exist. (30)

It's important to emphasize that amyloid aggregation properties are significantly different between the two principal Aβ forms, although both peptides aggregate into fibrils *in vitro*, Aβ1-42 does so more rapidly than Aβ1-40. The hydrophobicity of the residues at positions 41 and 42 is the major contributor to the enhanced amyloidogenicity of Aβ1-42 relative to Aβ1-40 (figure 5). That would be consistent with residues Ile41 and Ala42 taking place in the buried core of fibrils. Additionally these aminoacids have a good β-sheet propensity.

In Aβ1-42 these residues, together with Val39 and Val40 (which are also hydrophobic β-sheet formers), may form a β-strand at early stages of aggregation, hence lower the kinetic barrier for the aggregation of Aβ1-42 relative to Aβ1-40. (31) In addition the C-terminus of Aβ1-42 is more structured than that of Aβ1-40.

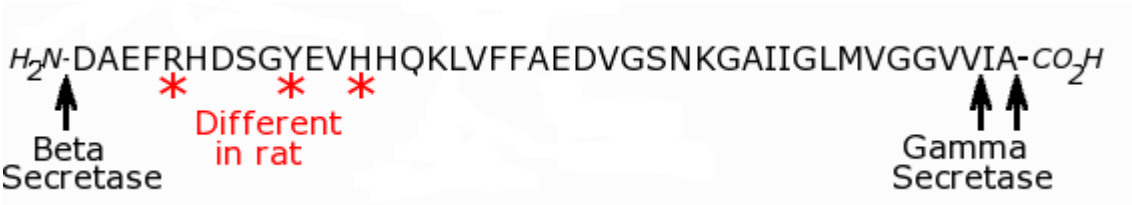

Figure 5. Aβ's aminoacid sequence

An interesting work asserts that Aβ1-40 inhibits Aβ1-42 oligomerization through the formation of a hetero-oligomer, typically a stable mixed tetramer via dimer condensation, composed of equal parts of Aβ1-40 and Aβ1-42. This suggests that Aβ1-40, in a healthy human brain, actually sequesters Aβ1-42 thus preventing its further oligomerization and formation of the putative dodecamer toxic form, and consequently potentially deterring the development of AD. (32)

Furthermore, increasing evidences suggest that the ratio of Aβ1-40 to Aβ1-42, rather than the total amount of Aβ, is an important determinant of aggregation, fibrillogenesis, and toxicity. (33)

Elucidation of the different mechanisms involved in aggregation, conformational transitions as well as in deep knowledge of fibrils and oligomers structure; will help us in the rational design of aggregation inhibitors.

For many years, the fibrillar Aβ assemblies, in analogy to what seen in amyloid plaques, have been considered the main responsible for the neurodegenation associated with AD. However, the quantity and temporal progression of amyloid plaques do not correlate well with the clinical evolution of the disease. (34)

An invariant and early feature of AD is the synapse loss and there is a strong correlation between the extent of synapse loss and the severity of dementia. Alterations in synaptic connectivity and/or strength have been observed in transgenic mouse models of AD before the appearance of senile plaques. (35,36)

In the past decade of research emerged a wide consensus pointing out the soluble non-fibrillar Aβ assemblies as the major cause of synapto toxicity in the early phases of the pathology. (8)

The pathogenic relevance of natural Aβ oligomers is supported by the observation that their formation is increased by expressing AD-causing mutations within APP or presenilin genes in recombinant cells.

Indeed, oligomers have been detected in CSF and in brain tissues of AD patients, where the level of soluble Aβ species appear to correlate with disease progression. (37-43) When micro-injected in living rats or added in vitro to hippocampal slices, natural oligomers of human Aβ are acutely toxic on synaptic functions. Soluble forms of Aβ have been shown to bind with high specificity to excitatory synapses and recently Steinerman et al. correlated AD symptoms with membrane-bound Aβ1-42 pools. (44)

Therefore to prevent the side effects of this amyloid aggregation pathway, research efforts should aimed at intervening at three different "steps" of the process, as shown in Figure 6:

1) Inhibiting Aβ production using small molecules or peptide/peptidomimetic which block the two secretases who produce Aβ from APP

2) Inhibiting the aggregation process itself

3) Increasing the clearance of the different aggregated forms using specific antibody

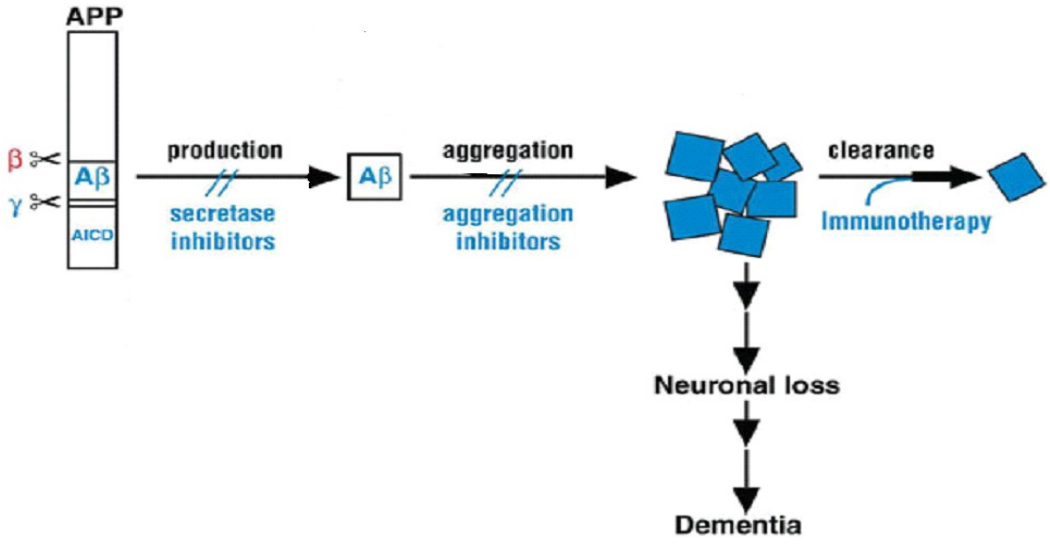

Figure 6. Different strategies to inhibit Aβ driven toxicity

1.3 Therapeutic strategies to inhibit amyloid aggregation process.

At present there is no cure for amyloidoses. Available therapeutic interferences are just symptomatic. (45)

Immune approaches have been tried for the treatment of AD, but the accompanying inflammatory process in the brain was severe enough for this approach to be abandoned. (46)

Also efforts have been made to inhibit the secretases responsible for the production of Aβ peptides but anyway these approaches have not been successful so far. Interference with the Notch signaling pathway is the greatest concern when developing gamma-secretase inhibitors; this make this protein not a good target to treat AD. (47)

Meanwhile Bace-1 has become an approved target in the discovery and development of medicines against AD because it is rate limiting for this disease process and a partial inhibition of this protein would result in a benign phenotype. (48)

The problem is that Bace1 seems to be a very challenging target for medicinal chemistry. First, Bace-1 has a large hydrophobic substrate-binding site designed to fit polypeptides, thus making it difficult to inhibit the enzyme with small non-peptidic compounds that have desirable drug-like characteristics. Ideally, Bace-1 inhibitor drugs should be molecules with a molecular weight <500, orally bioavailable, metabolically stable, intrinsically potent and highly selective for Bace-1. Compounds must also be hydrophobic enough to penetrate both plasma and intracellular membranes to gain access to the lumen of the compartment where the Bace-1 active site is localized. Finally, efficacious Bace-1 drugs would need to efficiently cross the blood-brain barrier and achieve a high concentration in the cerebral parenchyma. (49)

In such a scenario molecules able to prevent the basic molecular recognition process underlying the formation of Aβ early intermediates, would be the most valuable candidates for the treatment and the prevention of AD. A number of small molecules, carbohydrate and peptide-based inhibitors, have been shown to hinder Aβ aggregation and toxicity.

However to inhibit the formation of those toxic Aβ forms, understanding the details of the aggregation/fibrillation mechanism at the molecular level is crucial to develop an approach in which this process is inhibited.

Since numerous studies suggest that small oligomers, intermediate aggregate species formed during the first steps of the amyloid aggregation process, are the neurotoxic species in amyloid disease, agents that prevent or reverse their formation may in principle attenuate cytotoxicity. (50)

Many strategies to inhibit the amyloid aggregation process have been attempted. Some of them involve small molecules, carbohydrate (51) peptides and peptidomimetics. (52, 53)

1.3.1 Small molecules inhibitor

Various small molecules with specific primary targets have been shown also to interact with amyloidogenic protein and influence their aggregation. Tetracycline have been shown to prevent the formation of Alzheimer's amyloid aggregates beside the capacity to de-polymerize the Aβ1-42 fibril. (54) In addition having a well-defined antibiotic activity, tetracyclines are potent antiamyloidogenic agents. In the *C. elegans* model of AD, tetracyclines reduced the Aβ deposition, reduced the oxidative stress and delayed the disease onset. (55) The antifibrillogenic activity of tetracyclines appears to be different with respect to the protein involved.

Galantamine exhibited a dose dependent inhibition of aggregation of Aβ1-40 and Aβ 42. The cytotoxicity and apoptosis were significantly reduced. (56)

The chemical structure is important in the antiamyloidogenic property of these drug molecules in fact small variations can make the difference. Resveratrol has been observed to convert fibrillar intermediates into high molecular weight and unstructured aggregates. It did not accelerate the aggregation of monomers or soluble oligomers. Molecular dynamics simulations show that resveratrol interferes with the aggregation process by inhibiting the lateral growth and not the elongation. Inter sheet side chain interactions are interfered with resveratrol. (57)

Numerous small molecules are known to be efficient in preventing amyloid aggregation. Most of them have a central fused aromatic ring structure. More often they have many hydroxyl substitutions. The are many sources of these compounds.

A general remark describing their essential features will be made here. These compounds have the structural and chemical complementarity to interact with amyloid structures.

They are also good antioxidants since amyloid aggregation and oxidative damage are always involved in amyloid diseases. For those reasons compounds with antiaggregation and antioxidant activities are most probably better drug candidates. *In vitro* and *in vivo* experiments establish that these compounds can indeed reduce the aggregation of amyloids, sometimes reverse the aggregation and attenuate the oxidative damage. A various number of natural products such as curcumin, epigallocatechin gallate, extract from green and black tea, polyphenolic preparation from grape seeds and baicalein, a flavonoid extracted from the Chinese herb *Oroxylum indicum*, have been tested *in vitro* and *in vivo*. They have shown antifibrillation and antioxidant effects. (58)

1.3.2 Carbohydrate Inhibitors

Carbohydrate have been used as additives in protein folding experiments due to their well known effect in stabilize protein structure. The use of these sugars and their property has been extended to inhibit protein aggregation. This approach has been tried in many amyloid diseases such as Alzheimer, Parkinson and Huntington's diseases. The use of sugar in inhibiting protein aggregation consists in combining β-strand breaking property and enhancement of aqueous solubility. (58)

Trehalose has been established as protein's antistress molecule. It is used in protein folding experiments. It has a stabilizing role during heat denaturation or freeze-drying of proteins. The water substitution hypothesis is invoked in explaining the protective role of trehalose. The higher solubility and lower price make trehalose a tempting proposition as a therapeutic agent. Trehalose interacts through direct and solvent mediated interactions to weaken the inter-peptide interactions between Aβ chains. The surrounding layer of hydrophilic trehalose reduces the peptide-peptide hydrophobic interactions thereby reducing the aggregation. (59,60)

Glycodendrimers with sulfated glucosamine mimicking glycosaminoglycan suppress the fibril formation by Aβ peptides (Aβ1-42, Aβ1-40 and Aβ25-35). The effect depends on the nature of the carbohydrate moiety.

The acidic oligosaccharide sugar chain (AOSC), extracted from the brown algae Echlonia kurome, reduced the Aβ induced toxicity in the SH-SY5Y cell line and primarily cortical neurons. It interacts with monomeric Aβ and oligomeric Aβ. (58,61)

A stereoisomer of the sugar inositol, scyllo-inositol, has been shown to inhibit Aβ1-42 amyloid aggregation by directly interacting with the Aβ peptide. Many scyllo-inositol derivatives containing deoxy, fluoro, chloro and methoxy substitutions have been tested. The 1-deoxy-1-fluoro- and 1,4- dimethyl-scyllo-inositols were effective in inhibiting the Aβ1-42 fibrillation. This compound is going under clinical evaluations. It has been shown that scyllo-inositol, in CSF, decrease oligomeric Aβ1-42 concentration. Another sugar found in thermophilic microorganisms, alpha-d-mannosylglycerate (MG), has been observed to protect proteins against various structure-destabilizing conditions such as freezing, heat and drying. The efficacy of MG in preventing Aβ fibrillation and neurotoxicity in neuroblastoma cells has been shown as well. (58,61)

1.3.3 Peptide inhibitor

Peptides are molecules endowed with different characteristic that makes them interesting in drug discovery. Peptides are usually less toxic, more soluble and more specific than small organic molecules. Small peptide sequences encompassing the hydrophobic regions of the sequence of the aggregation-prone protein may interfere with the fibril formation process. (62)

This is like a competition between two molecules, one is the native protein/peptide and the other one is a smaller part of it. They compete to the same peptide segment, which forms the amyloid aggregate.

Since it is known that the major force driving amyloid aggregation is hydrophobicity, adding some charged residues to the ends of the recognition motif could be a disrupting element. (63)

Different works have show that at least three lysines are required as an appropriate disrupting element the compound (KLVFFKKKK) showed activity in altering fibril morphology and reducing cellular toxicity in vitro.

The compound with an anionic disrupting element KLVFFEEEE, has been observed having similar effects, while the neutral compound KLVFFSSSS was inefficient, suggesting that the charged nature of the disrupting element is critical. (63)

Different teams studied the incorporation of N methyl-amino acids into peptides as β-sheet disrupting elements. (64) The idea behind is that one side presents a hydrogen-bonding 'complementary' face to the protein, with the other side having N-methyl groups in place of backbone NH groups, thus presenting a 'blocking' face. N-methylated peptides corresponding to 16-22 and subsequently 16-20 sequence of Aβ have been studied. These peptides can prevent Aβ fibrils formation. N-methylation contributes in addition to make the peptides more resistant to proteolysis than normal peptides. Kapurniotu and colleagues synthesized an Api-28 analog constrained by an internal cycle between residues Lysl7 and Ala21. This modified peptide inhibited Aβ aggregation and cytotoxicity. (65)

β-sheet breakers peptides (BSB) have appeared years ago as the prototype class of compounds inhibiting Aβ aggregation. The β-sheet breaker approach uses the Aβ self-recognition motif (17-20) to achieve binding and specificity but, at sometime, replacing a residue important for forming β-sheets with an amino acid thermodynamically unable to fit inside β structure makes the aggregation process unfavorable. (66)

Valine at position 18 of Aβ plays an important role on stabilizing β -sheet folding in Aβ but it seems not to be necessary for self-recognition. Consequently, this amino acid has been replaced by proline, an aminoacid residue that due to of its particular chemical structure is an efficient β-sheet breaker. The β-sheet breaker peptide LPFFD has been developed by Soto and tested *in vitro*, in cellular model as well as *in vivo*. The *in vitro* activity was verified using both the Th-T binding assay, a commonly used fluorometric method to quantify amyloid, and qualitatively using electron microscopy to study the fibril morphology. Two animal models have been employed to monitor the activity of β-sheet breaker peptides in vivo. In both of them there were prevention of the formation of fibrillar lesion. (67)

The main problem of small peptides like the β-sheet breakers, it is that they are very easily degraded by peptidase and exhibit very short half-lives in vivo. (68)

For these reasons the synthesis of modified BSB peptides is necessary in medicinal chemistry.

Studies on the aggregation process of Aβ, identified the critical region involved in amyloid fibril formation; this has been mapped within the hydrophobic core at the residues 16-20 (KLVFF) of Aβ. (69) Designed peptides based on this self-recognition motif bind to the homologous sequence of Aβ thereby preventing its self-association.

Despite the good *in vitro* activity found for some of these compounds, their therapeutic usefulness is questioned due to their tendency to self-aggregate and to the risk of being incorporated into amyloid fibril.

Therefore, modified synthetic peptides based on the sequence of this central region of Aβ conjugated with the sugar trehalose, have been previously considered in our lab. (70) We used trehalose because it has been demonstrated to be effective in preventing the aggregation of numerous proteins including Aβ (71,72).

The antifibrillogenic ability of trehalose might stem from its preferential exclusion effect from the peptide surface. Consequently, threalose could stabilize the secondary structures of monomers, making the inter-peptide interactions/aggregation unfavorable. Yet, the thin hydration layer between Aβ and trehalose clusters around the peptide, thereby weakening the hydrophobic interactions between peptide chains. More recently a novel function of trehalose as autophagy activator has been reported. (73) This feature makes trehalose particularly interesting for application in protein-misfolding disease such as AD, in which the consequent enhancement of the clearance of damaged organelles and aggregates could be beneficial. It is expected that, the development of hybrid compounds may provide new molecules with improved properties that might sinergically increase the potency of their single moieties. As said before, earlier work was focused on the synthesis and neuroprotective activity of a novel class of trehalose conjugated LPFFD derivatives.

The disaccharide moiety was introduced in different regions of the aminoacid sequence (i.e. N- or C-Terminus or at the aspartic acid side chain) to endow these systems with optimal bioavailability in terms of higher stability toward proteolytic degradation within biological fluids and hence better opportunities for potential clinical trials. (70)

The C-terminus trehalose-conjugated peptide showed the highest stability toward proteolytic degradation in rat brain homogenate. (70)

Based on previous studies, in this PhD work we report further insight into the Aβ1-42 recognition process and neuroprotective action of the C-terminus trehalose-conjugated Ac-LPFFD-Th, a member of the above mentioned novel class of compounds.

We found that Ac-LPFFD-Th preferentially interacts with a specific region of the Aβ aminoacid sequence and interferes with the early events of Aβ's self-aggregation.

On the whole, our results suggest that hampering Aβ seeding capacity may constitute a viable and effective way to keep benign monomeric Aβ out from toxic oligomer formation. This would eventually lead to a protection against neurodegeneration and disease progression in AD. (70,74)

2. Materials and Methods

2.1 Peptide Synthesis

Peptides were assembled using the microwave-assisted solid phase peptide synthesis strategy on a Liberty Peptide Synthesiser. All Fmoc-amino acids were introduced according to the TBTU/HOBT/DIEA activation method. All syntheses were carried out under a 4-fold excess of amino acid. Removal of Fmoc protection during synthesis was achieved by means of 20% piperidine solution in DMF. The following instrumental conditions were used for each coupling cycle: microwave power 25Watts, reaction temperature 75◦C, coupling time 300 s.

The instrumental conditions used for the deprotection cycles were: microwave power 25 Watts, reaction temperature 75 ◦C, deprotection time 180 s. The acetylation was carried using a 20% acetic anhydride in DMF containing 5% DIEA.

Ac-LPFFD-NH2 and Ac-LFPDF-NH2 (Scrambled peptide)

These peptides were assembled using a Novabiochem TGR resin (substitution0.22 mmol/g). After the completion of the coupling cycles, the peptidyl resin peptide-TGR was treated with a mixture of Acetic Anhydride 20% in DMF for 1 h at room temperature to give the acetylated peptides. Then the peptides were cleaved from the resin using a mixture of Trifluoracetic acid (TFA) Triisopropyl-silane, water (95/2.5/2.5 v/v, 1h room temperature). The solution containing the free peptide was filtered, to remove the solid resin and concentrated *in vacuo*. The peptides were precipitated with cold diethyl ether, then filtered and dried under vacuum.

The resulting crude peptides were purified by RP-HPLC and characterized by ESI-MS. HPLC for Ac-LPFFD-NH2 [from 0 to 5 min isocratic elution with 100% A, then linear gradient from 0% to 30% B in 15 min, finally isocratic elution with 30% B; Rt = 28.37 min]. ESI-MS [obsd: m/z (M+ H)+ 679.3; (M + Na)+ 701.5; calcd for C35H46N6O8: 678.33].

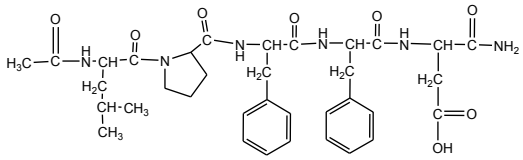

Ac-LPFFD-NH2

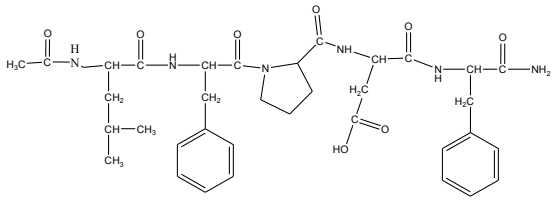

Ac-LFPDF-NH2 (Scrambled)

Ac-LPFFD-Th (Th-CT)

For the synthesis of the C-term derivate it has been used the Fmoc-Asp(Wang LL)-OAll resin (0.36 mmol/g, 0.1 mmol scale). After the completion of the synthesis of Ac-LPFFD(Wang LL)-OAll precursor, the dried peptidyl resin was treated with 10 ml of a CHCl3/AcOH/N-methyl-morpholine (37:2:1) mixture containing 0.4 mmol of Pd(PPh3)4, to selectively remove the allyl protecting group according to the resin provider (novabiochem). The resulting peptidyl resin with the free α-carboxy group of Asp was allowed to react with Th-NH2 (0.4 mmol) in the presence of HOBt (0.4 mmol), TBTU (0.4 mmol) and DIPEA (0.4 mmol) in DMF (5 ml) solution. The obtained trehalose-conjugated peptidyl resin was then treated with the TFA/TIS/H2O (95/2.5/2.5 v/v) mixture, the solution was filtered, concentrated under vaccum and the product precipitated with cold diethyl ether.

The obtained crude trehalose-peptide was purified by RP-HPLC and characterized by ESI-MS. HPLC [from 0 to 5 min isocratic elution with 100% A, then linear gradient from 0% to 35% B in 20 min, finally isocratic elution with 35% B; Rt = 28.0 min]. ESI-MS [obsd: m/z (M+Na)+ 1025.6; (M+K)+ 1041.1; calcd for C47H66N6O18)

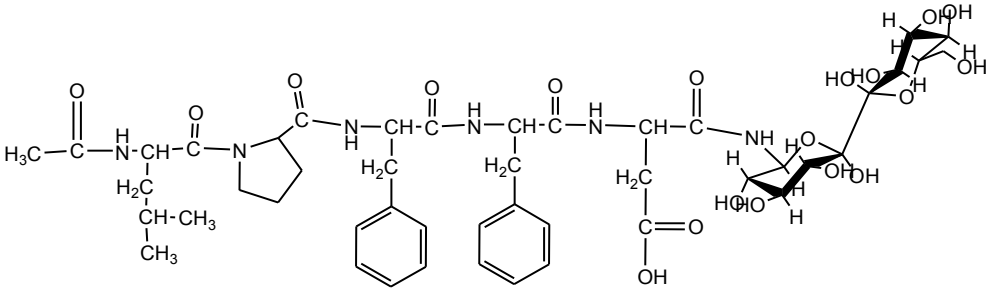

Ac-LPFFD-Th

2.2 Sample preparation

The Aβ1-42 lyophilized peptide was dissolved in TFA (1 mg/ml) and sonicated in a water bath sonicator for 10 min. Then the TFA was evaporated under a gentle stream of argon and 1 ml HEXA FLUORO ISOPROPANOL (HFIP) was added to the peptide. After 1 h incubation at 37°C, the peptide solution was dried under a stream of argon, the peptide film was dissolved in 2 ml HFIP, dried under argon stream to remove ANY remaining trace of TFA, again dissolved in 1 ml HFIP and frozen at -30 °C for 4 o 5 hours, then lyophilized overnight.

The lyophilized sample was dissolved in 10 mM phosphate buffer pH 7.4 to a concentration of 15 μM, ready for the DLS or Th-T measurements. In the case of biological experiments the lyophilized sample was dissolved in Dimethylsulfoxide (DMSO) at a 5mM concentration stock solution.

2.3 Thioflavin-T (Th-T) fluorescence assay for fibril formation

Amyloid growth kinetics were monitored by Th-T binding. A VarioSkan Flash from Thermo Scientific fluorescence 96-wells plate reader was used for the Th-T measurements. To minimize evaporation effects the multiwells plate was sealed by a transparent heat-resistant plastic film. Readings were taken every 10 min, after weak shaking for 10 s, over a window of time of 1400 min. Fluorescence excitation was at 440 nm and emission detected at 480 nm.

To minimize errors during sample preparation we freeze-dried the aliquots of monomerized Aβ1-42 and directly into each well of the plate. All Th-T experiments were carried out at pH 7.4, at 37 °C in 10mM phosphate buffer. The Th-T and Aβ1-42 concentration were 45 μM and 15μM respectively. Measuraments were carried out at 5 or 20 fold molar excess of the BSB peptides respect at to the Aβ1-42. All experiments were performed in quadruplicate.

2.4 Dynamic Light Scattering (DLS) experiments

DLS measurements were carried out on a Zetasizer Nano ZS (Malvern Instruments, UK) equipped for backscattering at 1738 with a 633 nm He–Ne laser. Aβ1-42 solutions (15 μm) were incubated at pH 7.4 in 10mM phosphate buffer at 37°C for 24 h either in the absence or in the presence of the peptide at the same molar ratio as for ThT assays. All DLS measurements were carried out at t=0h and t=24h and run using automated, optimal measurement times and laser attenuation settings.

The recorded correlation functions were converted into size distributions by using Dispersion Technology Software (DTS).

The software gives interpretations of the data collected for the sample such as intensity, volume and number distribution graphs, as well as statistical analysis for each. By using Mie theory the intensity distribution is converted into volume and number distributions.

2.5 Limited proteolysis and ESI experiment

Limited proteolysis experiments were performed to investigate the site of interaction between Aβ monomers and the beta sheet-breaker peptides. The experiments were carried out by co-incubating monomerized β-amyloid with the Ac-LPFFD-Th peptide at 37 °C in 10 mM ammonium bicarbonate buffer (pH 7.4) in the presence of trypsin (5 min) or insulin degrading enzyme (IDE, 60 min). ESI measurements were performed in presence of both the LPFFD and the Scrambled peptide in the same condition as well. The Aβ1-42 concentration was established at 50 μM in presence of equimolar concentration of the Ac-LPFFD-Th peptide. An enzyme to substrate ratio of 1:10 (w/w) with respect to Aβ was established. After digestion the samples were removed from the incubator and directly injected in the ESI source to immediately observe the proteolysis-derived fragments. The ESI-MS experiments were performed by using a Finnigan LCQ DECA XP PLUS ion trap spectrometer operating in the positive ion mode and equipped with an orthogonal ESI source (Thermo Electron Corporation, USA).

Sample solutions were injected into the ion source at a flow-rate of 5 μl/min, using nitrogen as a drying gas. The mass spectrometer operated with a capillary voltage of 46 V and capillary temperature of 250 °C, while the spray voltage was 4.3 kV.

2.6 NMR Interaction studies

NMR spectra were recorded at 298 K on a Varian^{UNITY} *INOVA* 600 spectrometer, equipped with a cold-probe.

The following samples were analyzed: 1) Ac-LPFFD-Th peptide (600 μM concentration), 2) Ac-LPFFD-Th peptide (600 μM concentration) plus Aβ1-40 (250 μM concentration); 3) Ac-LPFFD-Th peptide (600 μM concentration) plus Aβ1-40 (30 μM concentration). Lyophilized samples of Ac-LPFFD-Th peptide alone and in complex, were dissolved into the NMR buffer consisting of 50 mM sodium phosphate, 150 mM NaCl at pH=7.0 and 10% of D_2O (99.8% d, Armar Scientific, Switzerland); samples total volumes equal to 600 μL were implemented.

Excitation sculpting was used for water suppression (1); 1D [^{1}H] proton experiments were recorded with a relaxation delay d1=1.5 s and 64-128 scans; 2D [^{1}H, ^{1}H] TOCSY (Total Correlation Spectroscopy)

(2) (70 ms mixing time) and NOESY (Nuclear Overhauser Enhancement Spectroscopy) (3) (350 ms mixing times) experiments were typically recorded with 16-64 scans, 128-256 FIDs in the ω_1 dimension, 1024-2048 data points in the ω_2 dimension.

1D STD (Saturation Transfer Difference) experiments (4) were performed with samples 1, 2 and 3 as well; STD experiments were recorded with 4096 scans with an ensemble of Gaussian shaped pulses of 50 ms each with a 1 ms inter-pulse delay, for a total saturation time of 2 s and by alternating on-resonance irradiation at -1.0 ppm and off-resonance irradiation at 30 ppm. NMR data were processed with the software VNMRJ (Varian by Agilent Technologies, Italy). 2D NMR spectra were analyzed with NEASY, as implemented in Cara, (http://www.nmr.ch/).

2.7 Western Blot

10-12 mg of each unheated peptide sample were diluted in 4X Bolt LDS Sample Buffer without reducing agents or in Tricine Sample buffer**,** and size fractionated by SDS PAGE using pre-cast 4–12% Bolt Bis-tris gels (Life technologies) running in MES buffer or by native PAGE using 10-20% SDS polyacrylamide Tris-Tricine gels (Life technologies).

Peptides were transferred onto a 0.2 mm nitrocellulose membrane (Hybond ECL, Amersham Italia) using the semi-wet transfer unit Mini Blot Module (Life technologies). Membranes were blocked in Odissey blocking buffer (Li-COR Biosciences) and were incubated at 4°C o.n. with either 1:1,000 MAb 6E10 (against the amino-terminus of amyloid-ß Covance) or 1:500 mAb 4G8 (against the mid-region of amyloid-ß Covance) in 1:1 odissey bocking buffer/PBS-Tween. Secondary goat anti-rabbit labeled with IR dye 680 (1:20000 Li-COR Biosciences) or goat anti-mouse labeled with IRdye 800 (1:20.000 Li-COR Biosciences) were used at RT for 45 min. Hybridization signals were detected with the Odyssey Infrared Imaging System (LI-COR Biosciences). As discussed in the text, bands at 4 kDa correspond to Aß monomers whereas those at 8 kDa and at 12 kDa correspond to Aß dimers and Aß trimers, collectively named LDS/SDS-stable low MW Aß Os (due to the analysis method involving LDS in the sample buffer and SDS in the polyacrylamide gel), largely characterized in 7PA2 cells.

When required, membranes were stripped using New blot nitro stripping buffer (Licor) for 30–180 min at room temperature, depending on antibody affinity.

2.8 Pure neuronal cultures preparation

Cultures of pure cortical neurons were obtained from E15 rat embryos according to a well-established method that allows the growth of more than 99% pure neuronal population. (75)

Cortical cells were dissected, mechanically dissociated and seeded on medium consisting of DMEM F12 (1:1) supplemented with the following components: 10mg/ml bovine serum albumin, 10µg/ml Insulin, 100µg/ml trasferrin, 100µM putresceine, 20nM progesterone, 30nM selenium, 2mM glutamine, 6mg/ml glucose, 50U/ml penicillin and 50µg/ml streptomycin. Cortical cells were plated on 24-well plates pre-coated with 0.1 mg/ml poly-D-Lysine and incubated at 37°C with 5% CO_2 in a humidified atmosphere. Cytosine-β-D-arabinofuranoside (10µM) was added to the cultures 18 h after plating to avoid the proliferation of non-neuronal elements and was kept for 3 days before medium replacement.

Aβ1-42 monomers, Ac-LPFFD-NH_2 and Ac-LPFFD-Th peptides were added to mature neuronal cultures between 6 and 8 days *in vitro*.

2.9 Mixed Neuronal Cultures preparation

Cultures of mixed cortical cells, containing both neurons and glia, were obtained from rats at embryonic day of 17 and grown as described previously. (76)

Briefly, after dissection, cortical cells were plated onto Poly-D-Lysine coated 24-well plate in Eagle's minimal Essential medium (MEM) supplemented with 10% heat inactivated horse serum, 10% heat inactivated fetal bovine serum , 2mM glutamine and 15mM Glucose. After 5-7 days in vitro, glial cells division was inhibited by exposure to 10µM Cytosine-β-D-arabinofuranoside and the cells were shifted into a maintenance serum free medium. Medium was subsequently replaced twice per week. Mature cultures (14-16 days in vitro) were used for the study**.**

2.10 Assessment of NMDA toxicity in culture

Mixed cortical cultures at maturation were exposed to 300 μM NMDA for 10 min at room temperature in a HEPES-buffered salt solution (120mm NaCl, 5.4mM KCl , 1.8mM $CaCl_2$, 15mM Glucose, 20mM Hepes). Aβ monomers and the tested peptides were added in combination with NMDA . After extensive washing, cultures were incubated for 24hr into a maintenance medium. Neuronal toxicity was examined 24 h later by light microscopy and quantified after staining with trypan blue (0.4% for 5 min). Stained neurons were counted from three random fields/well.

2.11 MTT assay

Ac-LPFFD-NH_2 and Ac-LPFFD-Th peptides were applied to mature neuronal cultures between 6 and 8 days in vitro at final concentration of 100nM. During the experiment, cells were grown in absence of Insulin support and maintained for 48h at 37°C in 5% CO_2. To assess cell viability cells were incubated with [*3-(4,5*-Dimethylthiazol-2-yl)-2,5-Diphenyltetrazolium Bromide] (MTT 0,9 mg/ml final concentration) for 2h at 37°C. A solubilization solution containing 20% sodium dodecyl sulfate (SDS) was added and formazan production was evaluated in a plate reader at 560nm wavelength. To test the ability of trehalose-conjugated peptides to stabilize Aβ monomers, we incubated 100μM of fresh prepared monomeric Aβ at 4°C for 24h in the presence or in absence of Ac-LPFFD-NH_2 and its trehalose-conjugated derivative.

After incubation, a pure neuronal culture switched to an insulin deprived medium, was treated with peptide solutions at final concentration of 100nM. Cells were maintained for 48h and viability was assessed by MTT assay.

2.12 *In Vivo* assay

Animals and surgery

After habituation to the vivarium conditions, male C57BL/6J mice (3-4 months) underwent stereotaxic surgery under deep isoflurane anesthesia. One injection cannula connected via a catheter to a 5 ml Hamilton syringe was first aimed at the right lateral ventricle using the following coordinates: anteroposterior (AP) relative

to bregma, –1.0 mm; lateral (L) to midline, 1.3 mm; ventral (V) from the skull surface, -2.0 mm. A 4 µl solution of oligomeric forms of Aβos or Aβos +LPFFD-th or phosphate buffered saline (PBS) used as vehicle was infused at a rate of 0.5 µl/min with an injection pump controlling the syringe (Harvard Apparatus, Holliston, MA, USA). For mice infused with lidocaine (4% in artificial cerebrospinal fluid (aCSF), Sigma-Aldrich), bilateral guide cannulas were implanted into the dorsal hippocampus as previously described. (77) Lidocaine (0.5 ml per side) was delivered by means of cannulas connected to a 5 ml syringe mounted on a perfusion pump. Experimental procedures complied with official European Guidelines for the care and use of laboratory animals (directive 2010/63/UE) and were approved by the ethical committee of the University of Bordeaux (protocol A50120159).

Spatial recognition memory

The Y-maze two-trial procedure is routinely used to examine spatial recognition memory and takes advantage of the innate tendency of rodents to explore novel environments. (78) To increase its spatial cognitive demand, we adapted it to the 8-arm radial maze in which only three arms were used to form a Y-shape (90°-135°-135° between the arms). Each arm was 62 cm long and 12 cm wide and radiated from a central platform (32 cm in diameter). Training was composed of the exploration (encoding) phase and the recognition phase, which were separated by various inter-trial intervals (ITIs). During the encoding trial, one of the arms was blocked.

The mouse was positioned on the central platform of the maze and allowed to explore the two available arms during 10 min. During the recognition trial, the exploration time of each of the three arms was automatically recorded during a 5 min period with the entrance into an arm scored when the first half of the body was inside the arm.

Mice normally tend to explore the previously blocked arm (novel arm) of the maze more often than the previously accessible (familiar) ones. Discriminating the novel arm from the two familiar arms is thus considered as an index of spatial recognition memory. Memory performance was expressed as the percentage of time spent in novel arm ((seconds in novel arm)/(seconds in previously visited arms + seconds in novel arm) x 100).

3. Results

3.1 ThT assay

To compare the antiaggregating ability of the studied pentapepeptides, we carried out the rapid and specific assay based on the Th-T is fluorescence emission upon its binding to amyloid aggregates.

The results obtained by using the tested peptides in the presence of Aβ1-42 were compared to those of Aβ1-42 alone. Samples containing the peptides and Aβ at different molar ratios were co-incubated and co-lyophilized before dissolution in 200 μL of a 45 μM Th-T solution in 10 mM phosphate buffer at pH 7.4.

Interpretation of fluorescence data relies on the ability of Th-T to selectively detect amyloid structures, exhibiting a dramatic increase in fluorescent brightness. The more extended the aggregation is, the more intense is the emission of Th-T (λ= 480 nm); Th-T fluorescence originates only from the dye bound to amyloid substances because dye binding is linked to the presence of the cross-β structure. Th-T did not binds uniformly to the β-sheet surface, but preferentially interacts with channels formed by aromatic residues. (25)

We performed a Th-T assay of Aβ1-42 alone or in presence of the studied BSB peptides using different Aβ/BSB ratios. The Aβ1-42 alone as shown in figures 7, 8, 9 (blue curve) exhibits the classical sigmoid curve where after a lag-phase of approximately 300 minutes it starts to aggregate in fibrillar forms. It is clear from Figures 7, 8 and 9 that the Ac-LPFFD-Th shows the highest antifibrillogenic activity. This is clear already from figure 8, where at the Aβ/peptides ratio was 1:5, the LPFFD-Th is the most active. Looking at Figure 9, it can be also seen, apart a strong decrement in the whole fluorescence intensity with respect to Aβ, that the presence of this glycopeptide slows down the aggregation process through a lengthening of the lag phase.

In other words, the interaction between Aβ and the Ac-LPFFD-Th peptide not only greatly decreases the amyloidogenic process, but it seems that this peptide inhibits the early events of the aggregation process. In Figure 10 is shown the effect of the Ac-LPFFD-Th peptide at the three concentrations tested.

It is apparent a concentration dependent effect; in fact an almost flat curve is observed at the 1:20 molar ratio (300 μM), with no appearance of the exponential growth phase during the 21 hours of the kinetic assay.

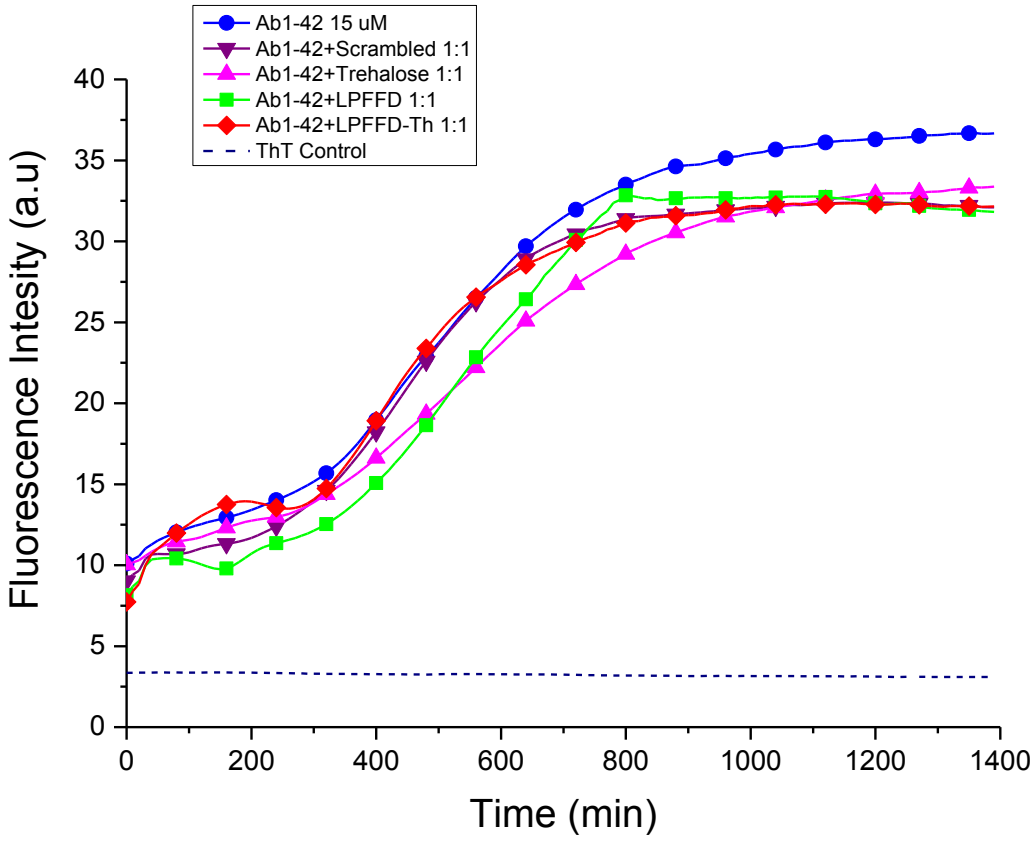

Figure 7. Fibril formation kinetics of Aβ1-42 monitored by Th-T fluorescence. The concentration of Aβ1-42 was 15 μM in 10mM phosphate buffer solution pH 7.4 at 37 °C. The measurements in presence of all of the peptides/Trehalose were carried out at equimolar concentration of the peptides/Trehalose with respect toAβ1-42.

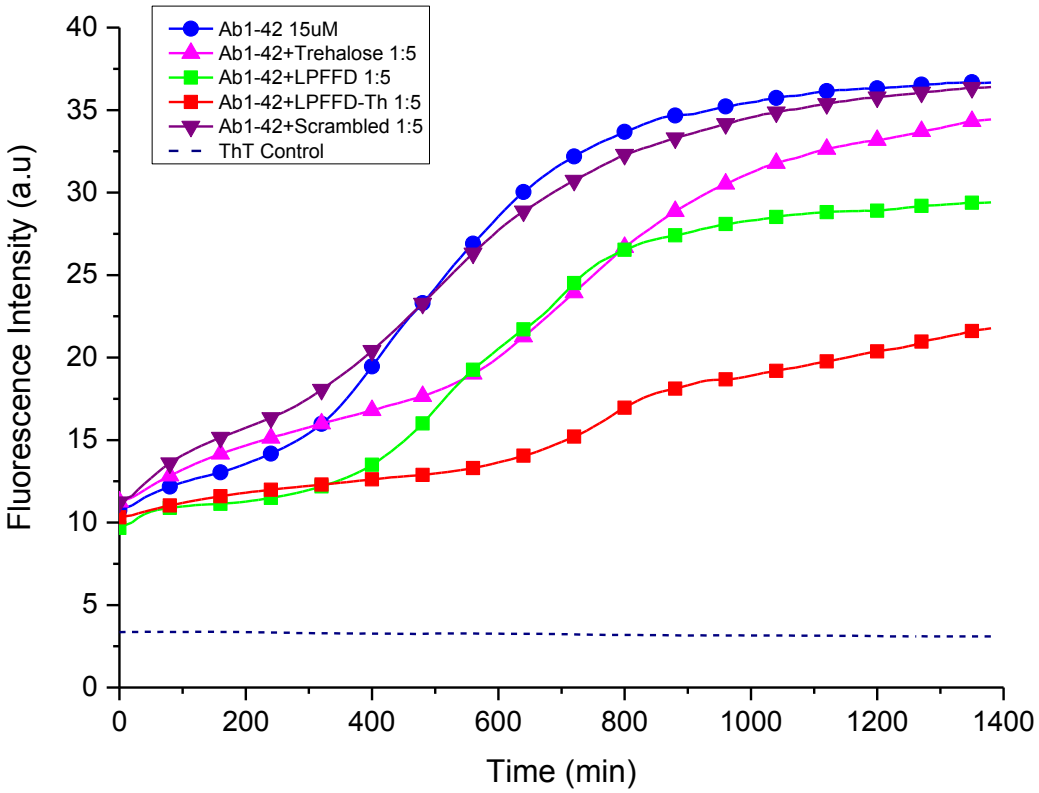

Figure 8. Fibril formation kinetics of Aβ1-42 monitored by Th-T fluorescence. The concentration of Aβ1-42 was 15 μM in 10mM phosphate buffer solution pH 7.4 at 37 °C. The measurements in presence of all of the peptides/Trehalose were carried out at 5 fold molar excess of the peptides/Trehalose with respect toAβ1-42.

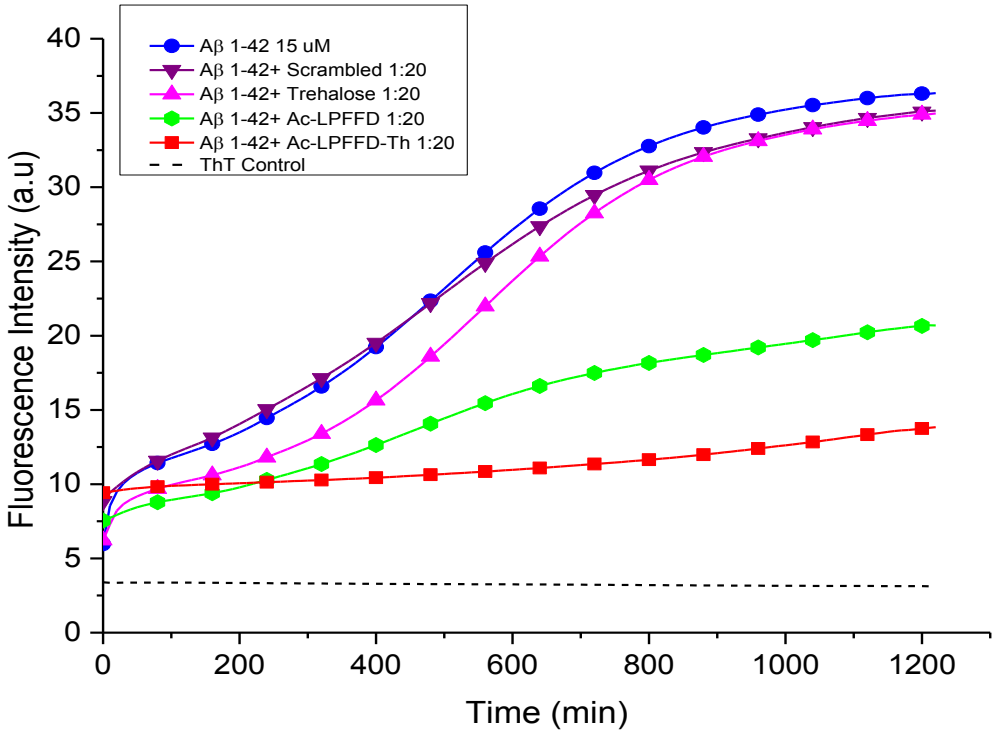

Figure 9. Fibril formation kinetics of Aβ1-42 monitored by Th-T fluorescence. The concentration of Aβ1-42 was 15 μM in 10mM phosphate buffer solution pH 7.4 at 37 °C. The measurements in presence of all of the peptides/Trehalose were carried out at 20 fold molar excess of the peptides/Trehalose with respect toAβ1-42.

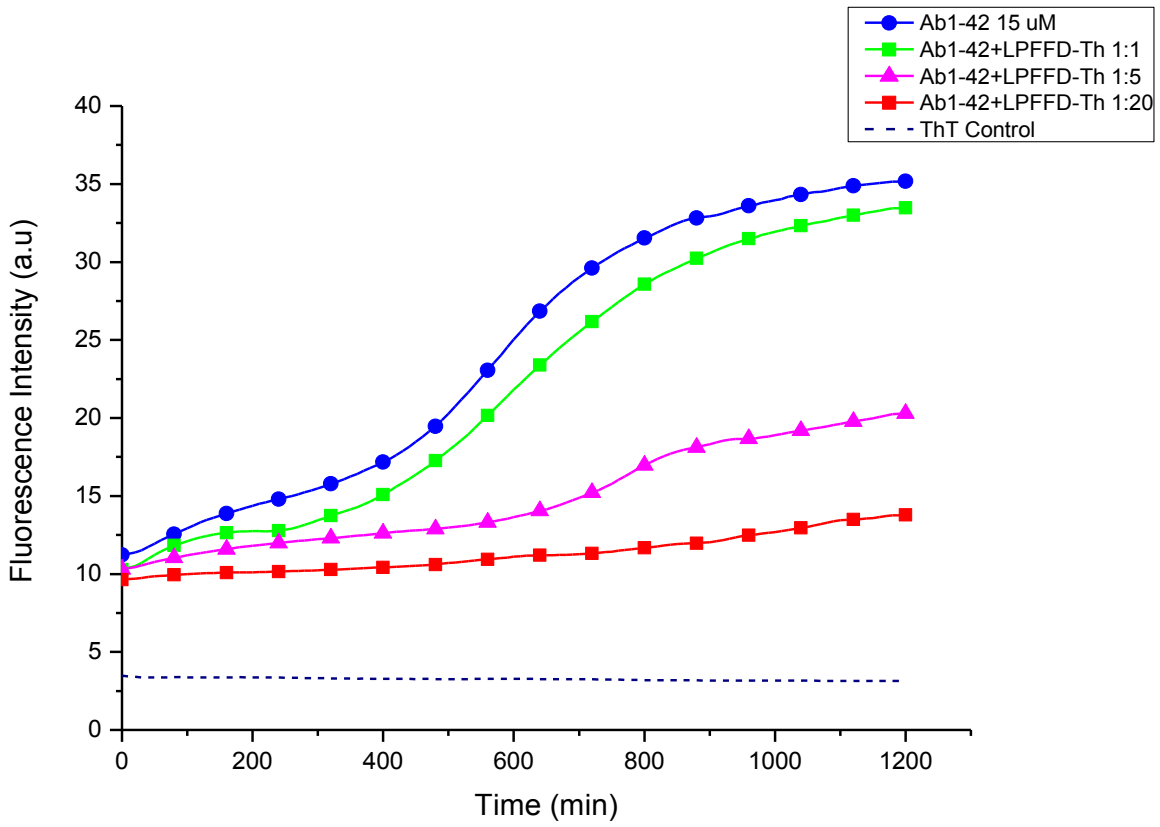

Figure 10. Fibril formation kinetics of Aβ1-42 monitored by Th-T fluorescence. The concentration of Aβ1-42 was 15 μM in 10mM phosphate buffer solution pH 7.4 at 37 °C. The measurements in presence of the peptide Ac-LPFFD-Th were carried out at 1,5,20 fold molar excess of the peptide with respect toAβ1-42.

As expected the scrambled peptide has little effect on the Aβ aggregation process, in fact the Th-T curve is similar to that one observed for Aβ alone (Figure 7,8,9).

Notably, trehalose alone shows a slight effect in slowering the lag phase of Aβ aggregation resulting in a decreasing on the aggregates formation (Figure 7,8,9).

We wanted also to investigate if the fibrillation inhibition effect observed on Aβ1-42 from Ac-LPFFD-Th was specific. For this reason we used another amyloidogenic peptide, IAPP (Islet Amyloid Polypeptide). This 37 aminoacids peptide is involved in type II diabetes mellitus where it is found as the mayor component in amyloid deposit in pancreatic β-cell of patients affected with T2DM.

hIAPP is an amyloidogenic peptide which shows about 25% sequence identity and 50% sequence similarity with Aβ peptide and morphology of amyloid fibrils for these reason we used hIAPP to perform a ThT assay in presence of our beta-sheet breaker peptide. (79,80)

From the ThT fluorescence data we can observe ~~as~~ how hIAPP 20 μM shows a fast fibrillation process with a lag phase of a bit less than 4h in agreement with our previous work. (80)

hIAPP, in the presence of Ac-LPFFD-Th 20 molar fold in excess, does not inhibit the hIAPP fibril formation, but rather promotes hIAPP aggregations. (Figure 11)

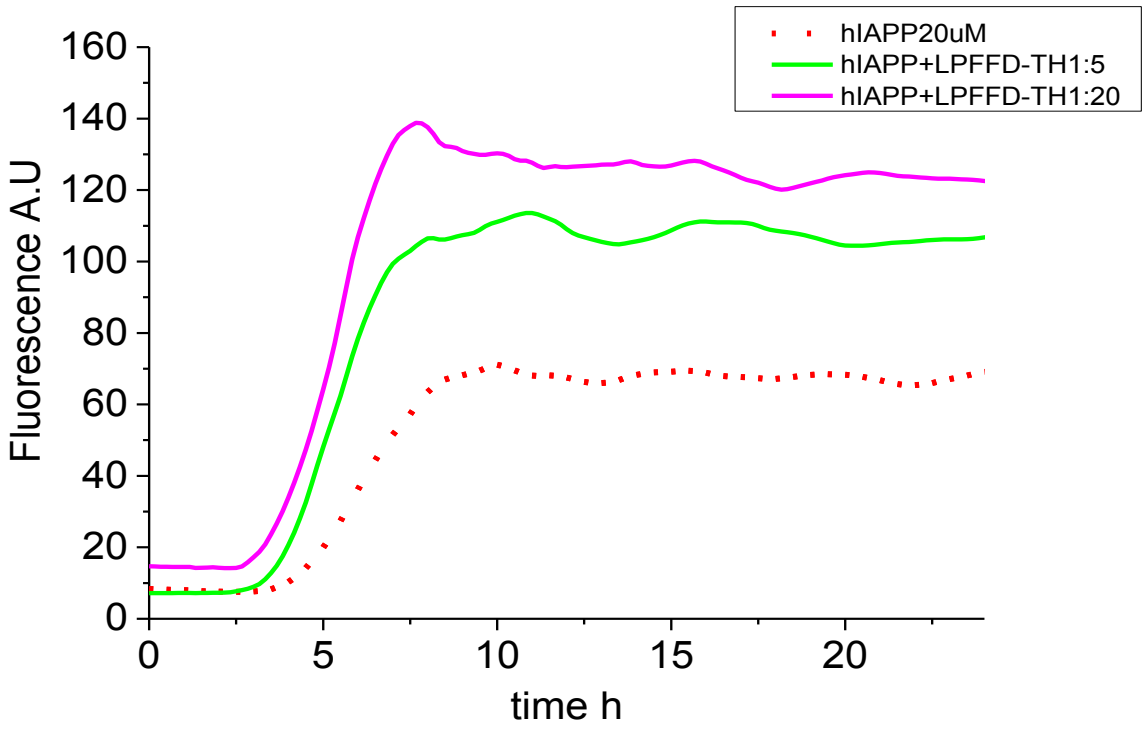

Figure 11 Fibril formation kinetics of hIAPP monitored by Th-T fluorescence. The concentration of hIAPP was 20 μM in 10mM phosphate buffer solution pH 7.4 at 37 °C. The measurements in the presence of the peptide Ac-LPFFD-Th were carried out at 5,20 fold molar excess of the peptide with respect to hIAPP.

3.2 Dynamic light scattering

To further examine the influence of Ac-LPFFD-Th on the aggregation process of Aβ1-42, we resorted to DLS measurements. This allowed us to determine the average size of the aggregates and to follow the evolution of the aggregates over time, either in the absence or in the presence of 20 fold molar excess of the beta sheet breaker peptide Ac-LPFFD-Th. Data were collected at t=0h and t=24h The freshly prepared Aβ1-42 sample (t=0h) displays a composite profile of small and medium size aggregates (Figure 12). Since the particle scattering intensity is proportional to the molecular size of aggregated forms, the analysis of the number (as well as the volume) of the scattering objects indicates that the actual abundance of the larger particles (>100 nm) is significantly lower than the one of the smaller particles with an hydrodynamic radius (*R*H) around 10 nm (Figure 13).

The progression of Aβ aggregation was analysed after 24h and the presence of larger aggregates was observed (Figure 12). In particular, the inspection of the respective DLS (number) profile indicated the formation of particles with increased *R*H values (> 50nm) as the major scattering objects (Figure 13). The data collected after 24 h in the presence of Ac-LPFFD-Th indicated that the pentapeptide-conjugate significantly reduced the formation of Aβ1-42 larger aggregates (Figure 12, curve profile c). Notably, after 24h the majority of the scattering particles in solution displayed *R*H values smaller than 10 nm, (Figure 13). It should be mentioned finally that the peptide Ac-LPFFD-Th did not provide evidence of aggregated species anytime.

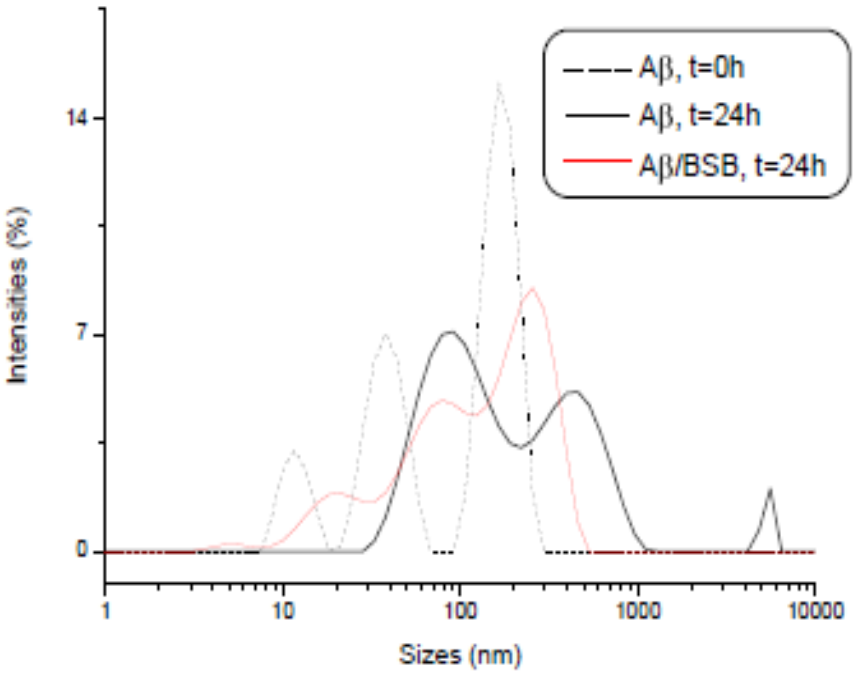

Figure 12. DLS. Intensities (%) as function of Hydrodynamic ratio of Aβ1-42 alone or in the presence of 20 molar fold excess of Ac-LPFFD-Th in Phosphate buffer 10 mM at 37°C, pH 7,4.

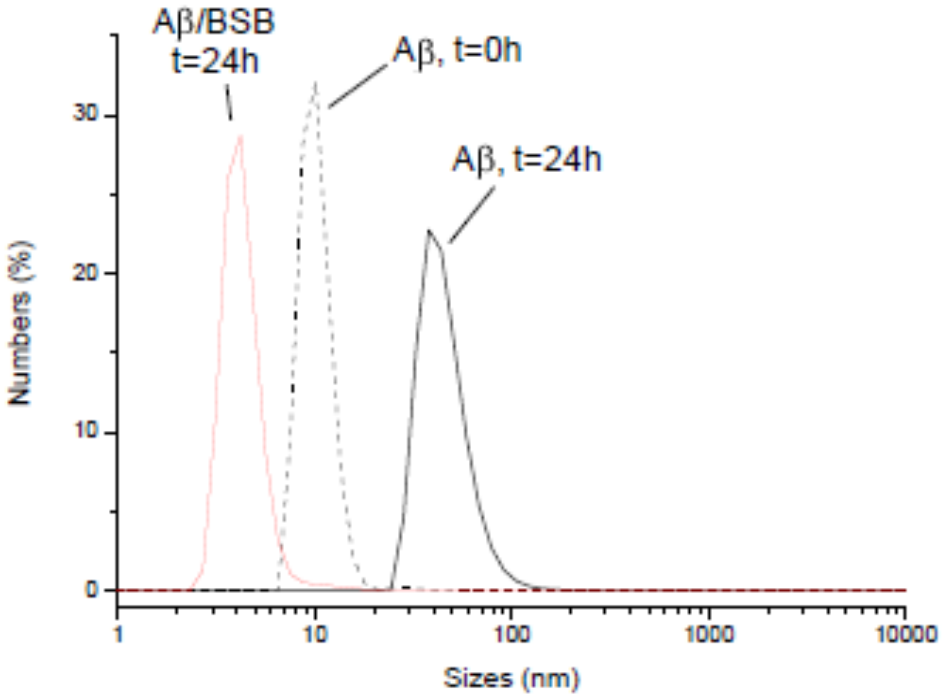

Figure 13. DLS. Numbers (%) as function of Hydrodynamic ratio of Aβ1-42 alone or in the presence of 20 molar fold excess of Ac-LPFFD-Th in Phosphate buffer 10 mM at 37°C, pH 7,4.

3.3 Recognition of the full-length Aβ monomeric form (ESI and limited proteolysis)

In an attempt to identify the Aβ1-42 aminoacid sequence which might constitute the binding epitope for Ac-LPFFD-Th, an array of limited enzymatic proteolysis experiments, followed by ESI-MS analysis, were performed in our laboratory. The ESI-MS spectrum carried out on intact Aβ1-42 50 μM in the presence of equimolar Ac-LPFFD-Th, showed, beside the expected peak distribution of the single peptides, the presence of multi-charged mass adduct peaks with mass values corresponding to the Aβ42/ Ac-LPFFD-Th non covalent complex (Figure 14).

After digestion with insulin degrading enzyme (1:10 w/w, 60', 37°C), the ESI-MS spectrum revealed, along with the degradation profile of Aβ1-42, the presence of a single-charged mass peak at 1636.4 m/z. This observation strongly supports the formation of a non covalent complex occurring between the "QKLVF" sequence (aminoacid region 15-19) of the Aβ1-42 and the Ac-LPFFD-Th peptide (mass calculated: 1635.82 Da) (Figure 15).

The results obtained upon incubation of the Aβ1-42/AcLPFFD-Th system with Trypsin were not dissimilar (1:10 w/w, 5', 37°C). In this case, the formation of double-charged mass adducts at 1164.5 m/z and 1789.9 m/z were observed. These signals can respectively be identified as the non covalent complexes of Ac-LPFFD-Th with the 17-28 and 17-42 aminoacidic fragments of Aβ1-42 (mass calculated: 1164.96 and 1790.76 Da respectively) (Figure 16).

From the above experiments we concluded that the 16-20 aminoacid region of Aβ1-42 might represent the major binding site targeted by the Ac-LPFFD-Th peptide.

Further support to this conclusion was provided by the use of the Aβ16-28 fragment, that after the proteolysis with IDE carried out in the presence of Ac-LPFFD-Th, gave a molecular peak adduct with the "KLVF" peptide fragment that is encompassed within the aminoacidic region "16-19". (figure 17). Finally, the scrambled peptide Ac-LFPDF-NH_2, was also tested to verify the occurrence of a sequence specific recognition. The ESI-MS spectrum recorded after the IDE catalyzed Aβ1-42 proteolysis, in the presence of Ac-LFPDF-NH_2, did not show any mass adduct with the expected peptide fragments (figure 18).

This result supports the hypothesis that the recognition process between Aβ monomers and the beta sheet breaker (BSB) peptide is specifically sequence-dependent and a random arrangement of the five aminoacids renders the matching unfavorable.

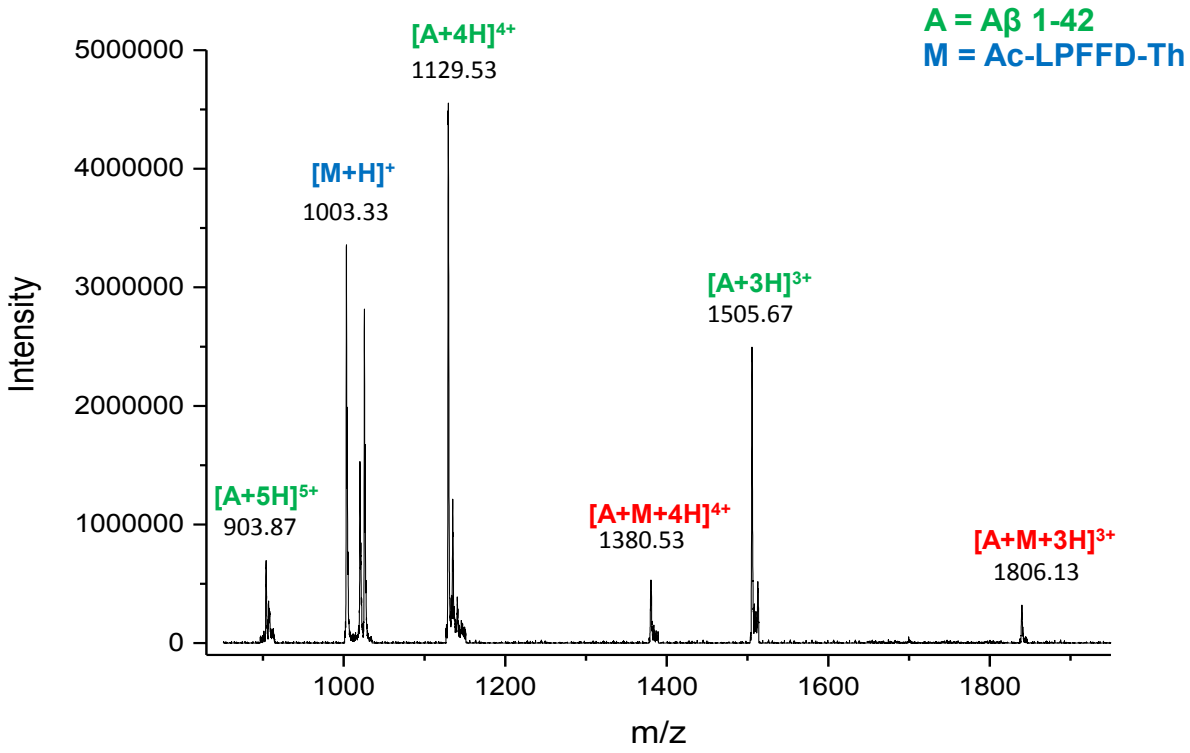

Figure 14. ESI-MS mass spectrum of Aβ1-42 50μM in presence of the peptide Ac-LPFFD-Th (ratio 1:1) in 10mM NH_4HCO_3 buffer. The numbers above the peaks indicate the m/z with superimpose the positive-charge state of the ions. Green Aβ1-42. Blue Ac-LPFFD-Th. Red molecular peak molecular peak Adducts.

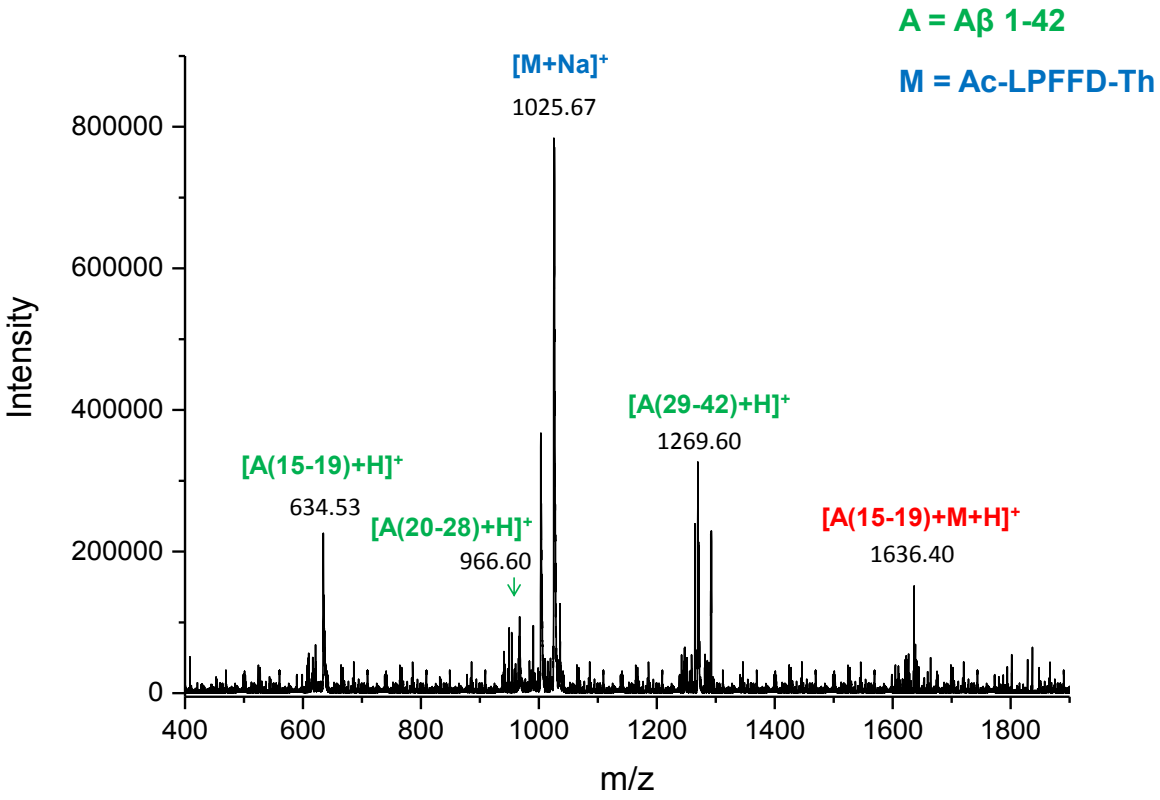

Figure 15. ESI-MS mass spectrum of Aβ1-42 50μM in presence of the peptide Ac-LPFFD-Th (ratio 1:1) in 10mM NH_4HCO_3 buffer, after digestion with IDE at 37°C for 60 min. The numbers above the peaks indicate the m/z with superimpose the positive-charge state of the ions. Green Aβ1-42. Blue Ac-LPFFD-Th. Red molecular peak Adducts.

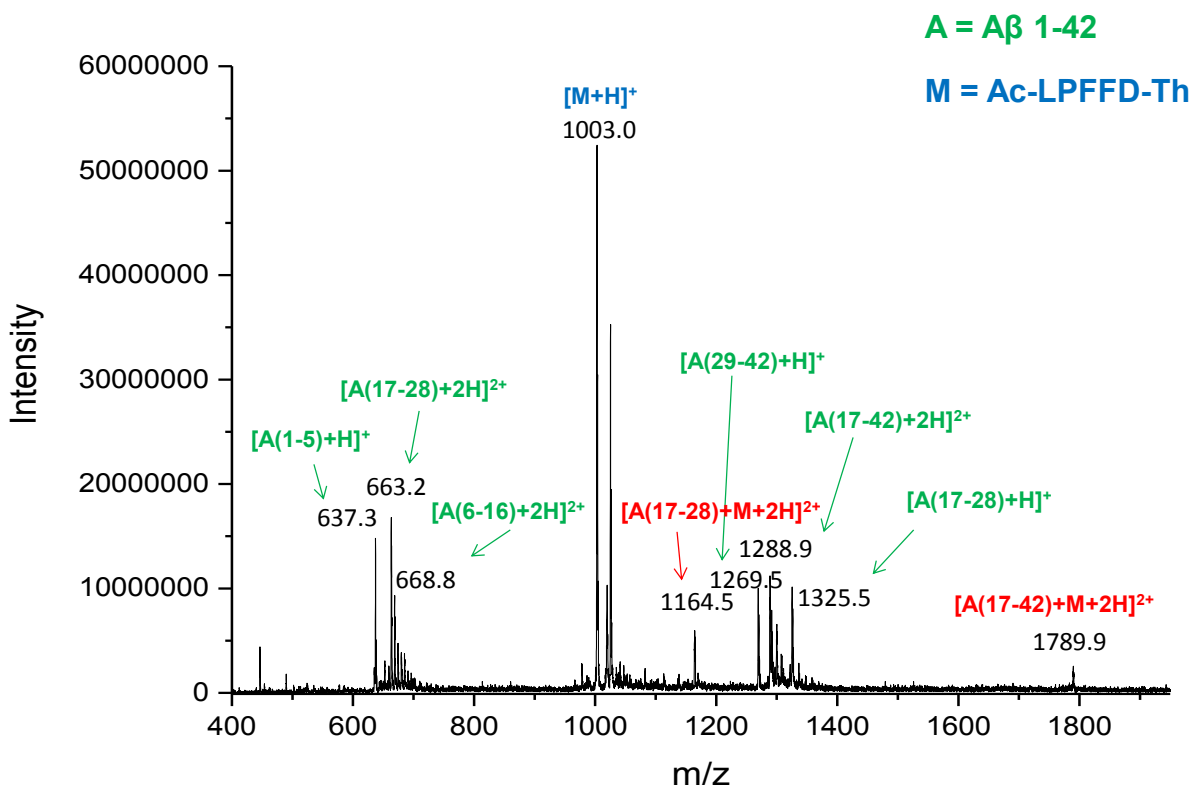

Figure 16. ESI-MS mass spectrum of Aβ1-42 50μM in presence of the peptide Ac-LPFFD-Th (ratio 1:1) in 10mM NH_4HCO_3 buffer, after digestion with Trypsin at 37°C for 5 min. The numbers above the peaks indicate the m/z with superimpose the positive-charge state of the ions. Green Aβ1-42. Blue Ac-LPFFD-Th. Red molecular peak Adducts

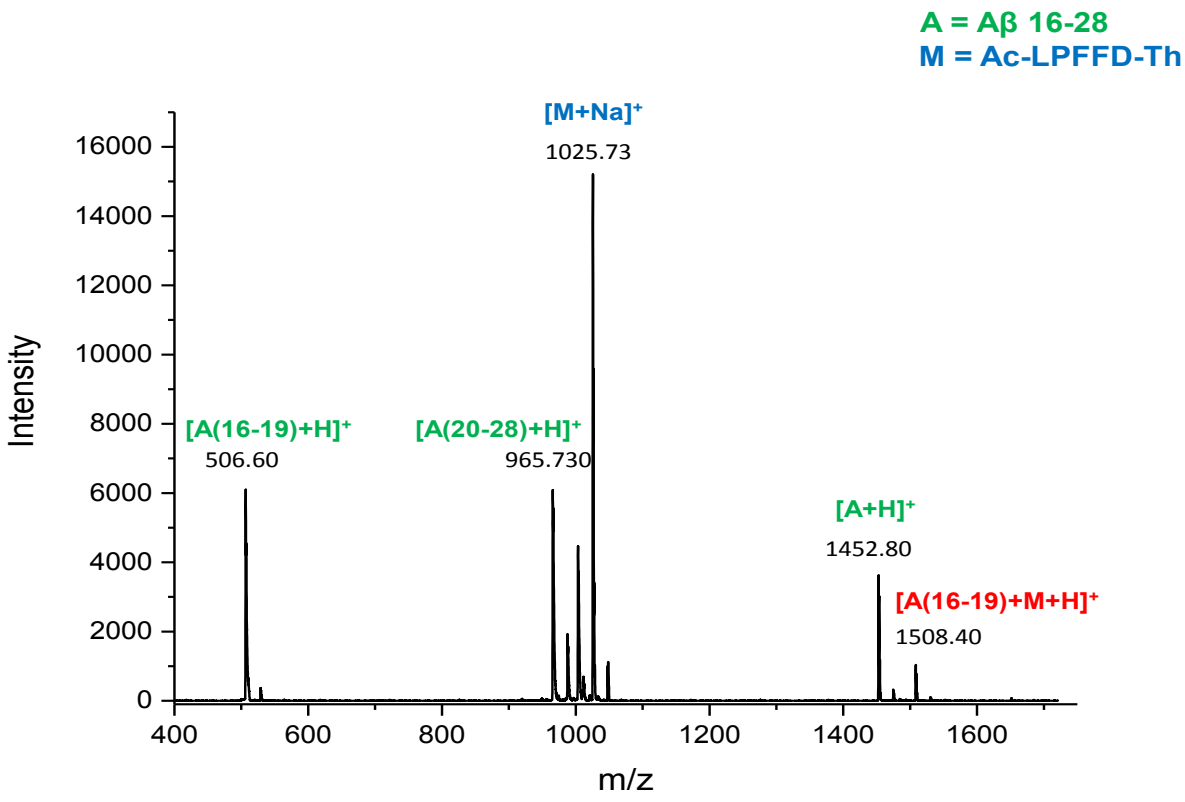

Figure 17. ESI-MS mass spectrum of Aβ16-28 50μM in presence of the peptide Ac-LPFFD-Th (ratio 1:1) in 10mM NH_4HCO_3 buffer, after digestion with IDE at 37°C for 60 min. The numbers above the peaks indicate the m/z with superimpose the positive-charge state of the ions. Green Aβ1-42. Blue Ac-LPFFD-Th. Red molecular peak Adducts.

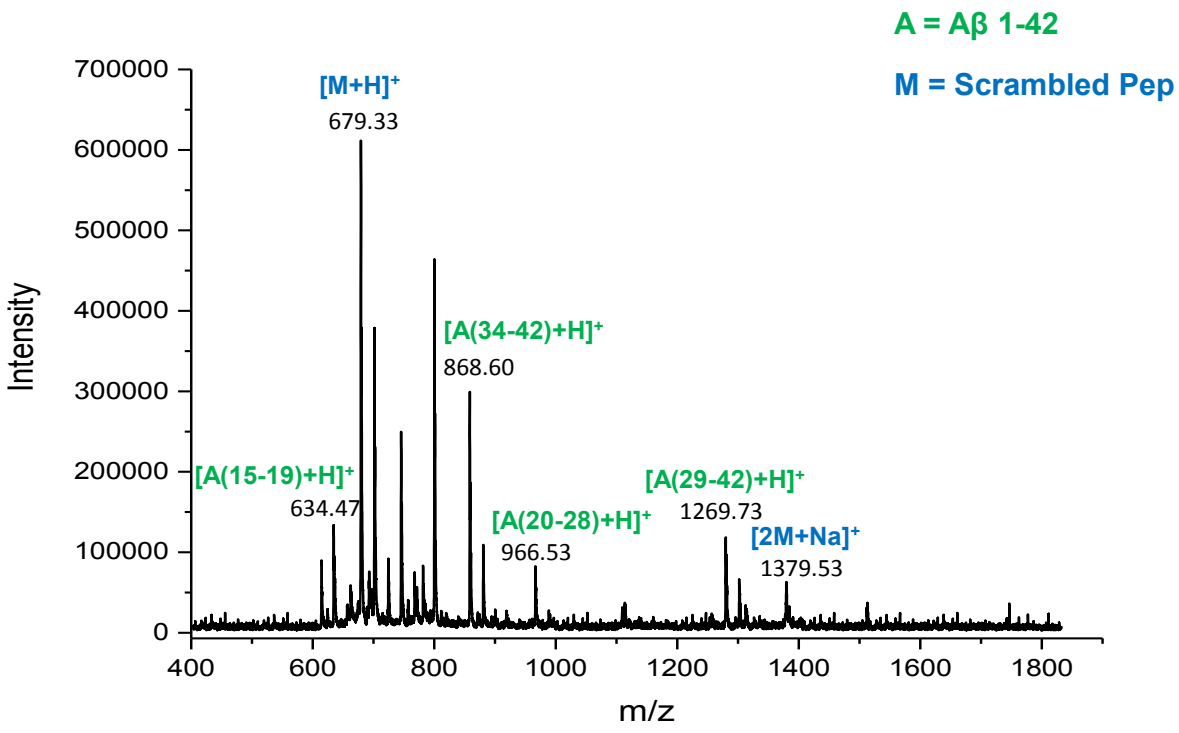

Figure 18. ESI-MS mass spectrum of Aβ1-42 50μM in presence of the Scrambled peptide (ratio 1:1) in 10mM NH_4HCO_3 buffer, after digestion with IDE at 37°C for 60 min. The numbers above the peaks indicate the m/z with superimpose the positive-charge state of the ions. Green Aβ1-42. Blue Scrambled peptide.

In our mass spectrometry study in a first step we observed the adduct between the Ac-LPFFD-Th and Aβ polypeptide. Furthermore proteolitic experiments using Insulin Degrading Enzyme (IDE) and Trypsin have been performed to show as the Ac-LPFFD-Th peptide is always able to recognize the hydrophobic core 16-20 of Aβ peptides. This hydrophobic driven recognition process seems to be qualitatively weak also because hydrophobic interactions are typically weakened in the gas phase typical of an ESI ionization chamber. (81)

The recognition process is sequence specific in fact with the scrambled peptide there are no adduct observed. A possible explanation about the fact that this bi-molecular interaction between monomeric Aβ and Ac-LPFFD-Th is observed only in ESI experiments could be due to the fact that in a typical ESI experiment aggregated forms are difficult to be detected.

3.4 NMR Interaction studies between Ac-LPFFD-Th with Aβ16-28 and Aβ1–40

The ESI-MS study provided experimental evidence of a direct interaction between the Aβ1−42 monomer and the Ac-LPFFD-Th. However from these experiments no data could be obtained about a possible interaction of the Ac-LPFFD-Th with aggregated forms of Aβ1−42. NMR experiments might provide better information about this last event.

We performed different NMR experiments with Ac-LPFFD-Th in the presence of either the fragment Aβ16-28 or Aβ1−40. We used these peptides because the first one includes the potential interacting sequence KLVFF and since it is relatively small it is easier to study by NMR. The Aβ1−40 was used instead of Aβ1−42 because its higher solubility and slower aggregation kinetic.

The 1D [^{1}H] spectrum of the peptide Ac-LPFFD-Th contains rather sharp lines so there is no evidence of aggregation of the peptide alone also at this high concentration (1mM) (Figure 19).

The process of resonance assignments has mainly been achieved through analysis of the 2D [^{1}H, ^{1}H] TOCSY experiment. The [^{1}H, ^{1}H] NOESY spectrum presents only a few very weak cross-peaks, as well as the ROESY experiment; this is a strong indication of high peptide flexibility.

Chemical shift deviations from random coil values (CSD) were evaluated with the method recently proposed by Kjaergaard, M**.** et al. (82) by keeping into account effects by neighboring amino acids. CSD values do not present a single particular trend characteristic of one ordered secondary structure element (figure 20).

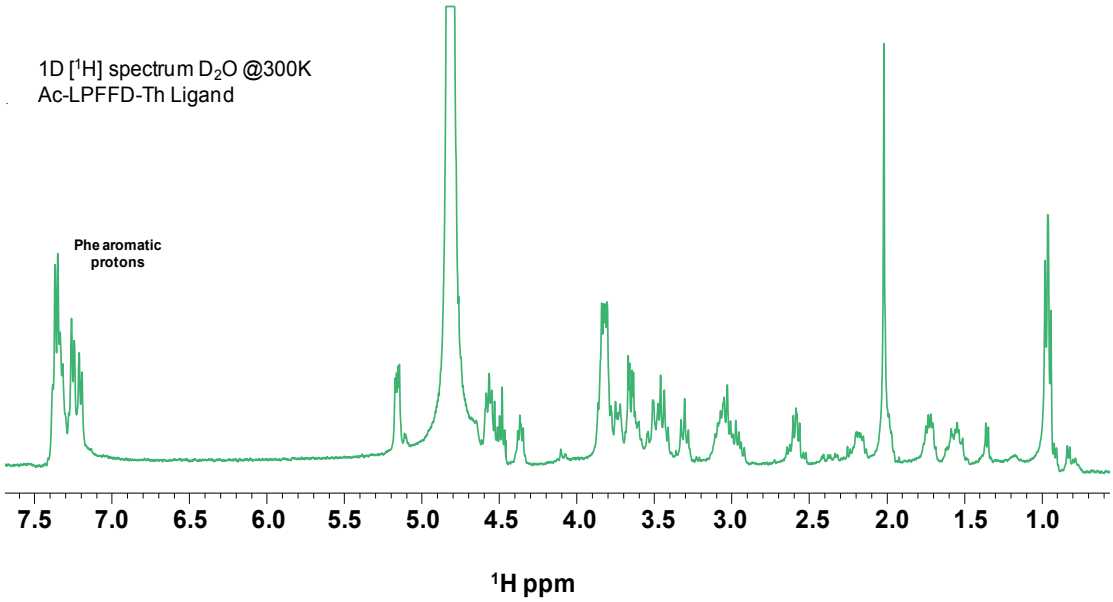

Figure 19. 1D [^{1}H] spectrum of the peptide Ac-LPFFD-Th 1 mM in phosphate buffer at 27°C.

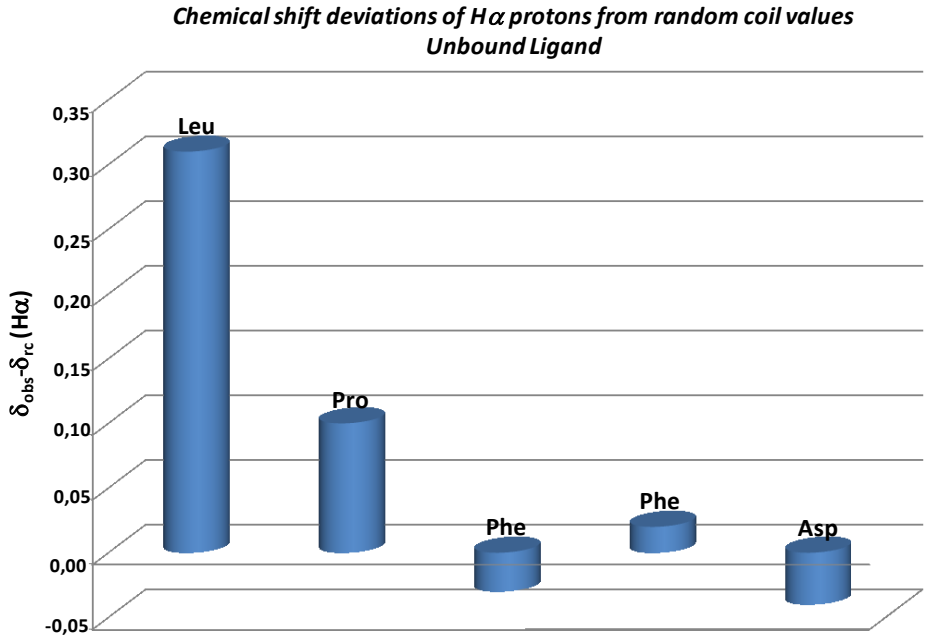

Figure 20. Chemical shift deviations from random coil values (CSD) of the peptide Ac -LPFFD-Th 1 mM in phosphate buffer at 27°C

The 1D [^{1}H] spectrum of the peptide Aβ16-28 was acquired and as we can see from figure 21B a certain broadening of the resonances was evident, so we cannot exclude the presence of small aggregates. Resonance broadening increases in the spectrum of the complex (figure 21C). Resonance assignments are rather close to those observed in previous NMR studies of Aβ1–42. (83)

Chemical Shift Deviations (CSD) from random coil values related to the Hα protons of Aβ16-28 are reported below (figure 22). CSD are also for this peptide small and then not really featuring a completely ordered conformation. Positive deviations, that are generally hallmarks of β-extended structures, are found in the N-terminal part between Leu2 and Phe5.

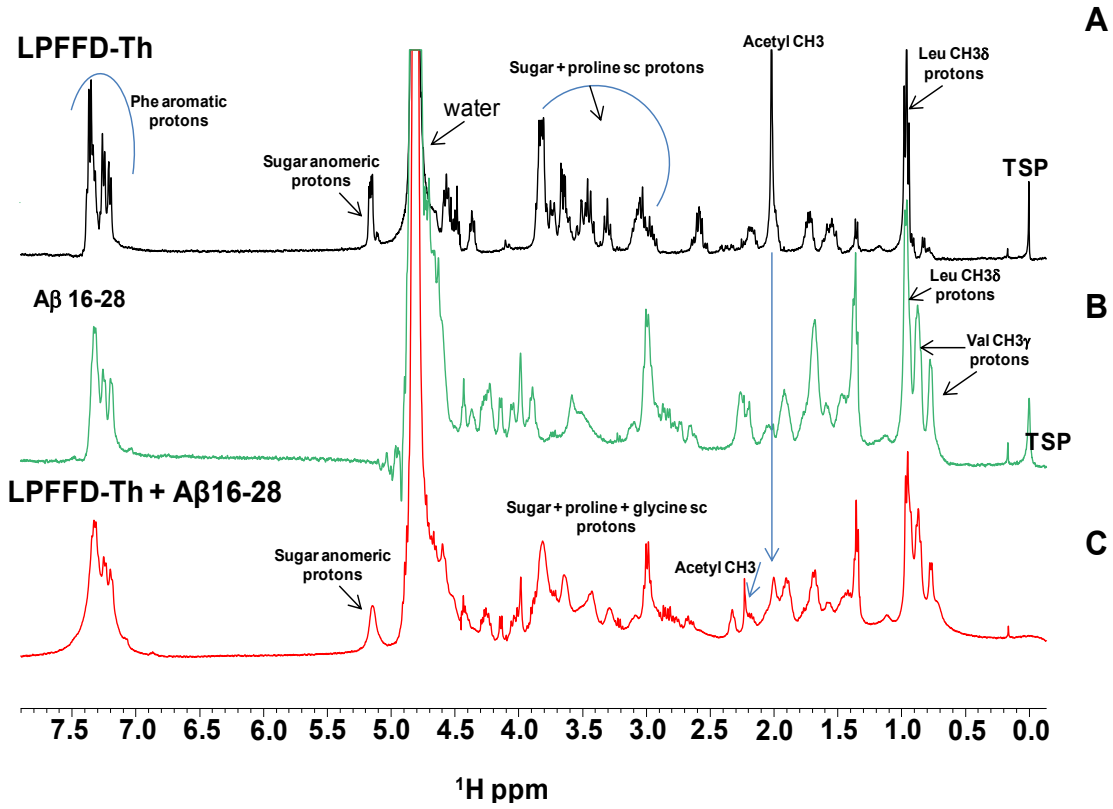

Figure 21. A) 1D [^{1}H] spectrum of the peptide Ac-LPFFD-Th 1 mM in phosphate buffer at 27°C.
B) 1D [^{1}H] spectrum of the peptide Aβ16-28 1 mM in phosphate buffer at 27°C.
C) 1D [^{1}H] spectrum of the peptide Ac-LPFFD-Th 1mM in presence of Aβ16-28 1mM in phosphate buffer at 27°C.

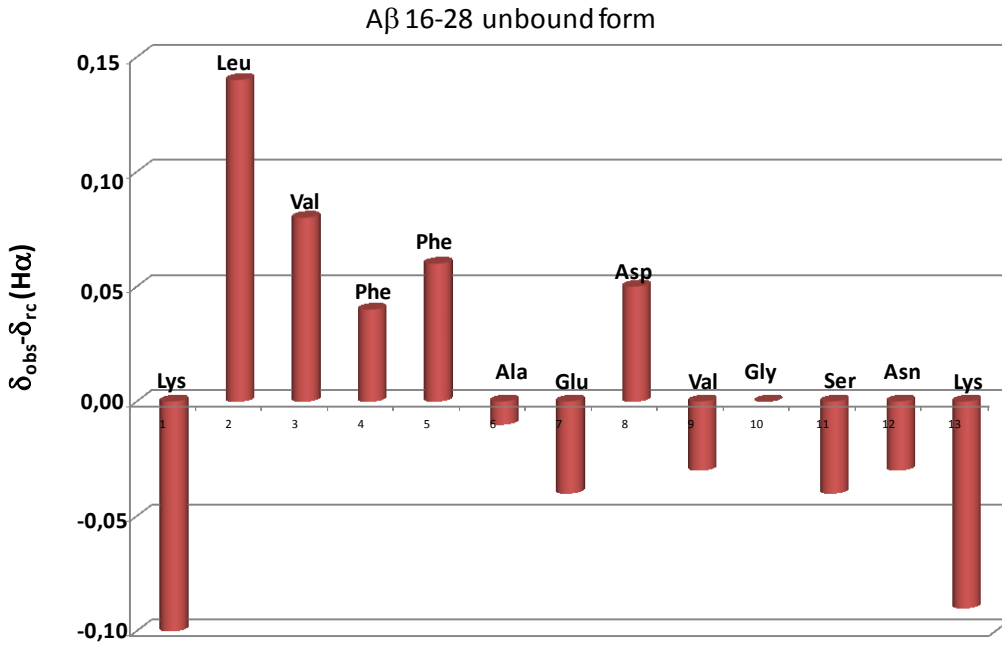

Figure 22. Chemical shift deviations from random coil values for Hα protons of Aβ16-28

In the 2D NOESY spectrum of Aβ16-28 we can see a few weak NOEs indicating at least a partial β-structure formation and thus possible aggregation. (We exclude formation of very large species for which we would expect much large broadening of the resonances and "very poor NMR spectra") (figure 23). In the NOESY spectrum we can see weak intra or intermolecular Hα-Hα NOEs suggesting an organized fibrillar structure composed of parallel β units.

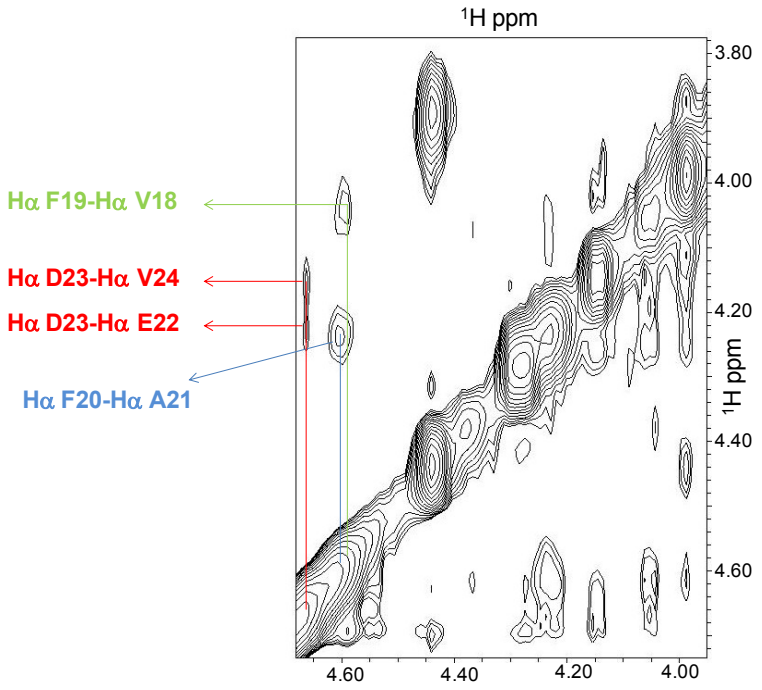

Figure 23. Hα region of the 2D [^{1}H; ^{1}H] NOESY spectrum of Aβ16-28. The Hα protons were keep into account because easy to recognize in the NMR spectrum. The contacts Hα G25-Hα S26 and Hα L17-Hα V18 are also neat (not reported in Figure). These NOEs suggest a partial β-structure.

Furthermore we performed NMR studies of the complex Ac-LPFFD-Th / Aβ16-28 (ratio 1:1). In Figure 21 the comparison of the 1D [^{1}H] spectra of Ac-LPFFD-Th alone, Aβ16-28 alone and their mixture is reported. The NMR signals are rather broad in the complex in comparison with those corresponding to the Ac-LPFFD-Th and Aβ16-28 peptide alone.

For example NMR lines corresponding to sugar protons became very large; all signals mainly from the ligand became rather large so that we have problems in trying to assign all resonances.

The N-terminal part of Ac-LPFFD-Th peptide seems to be particularly involved in the interaction with Aβ16-28 mainly including Leu1 and Pro2 residues. For example from a close inspection of the first (figure 21A, black) and last (figure 21C, red) 1D spectra, it is clearly shown that the protecting acetyl group is highly flexible.

Interestingly from the NOESY of the complex, it seems like that the Ac-LPFFD-Th peptide, when in presence of Aβ16-28, makes a "bend" and the sugar protons have intra-molecular NOE contacts with Leu1 and Pro2 (figure 24).

Interestingly it looks like the Qγ2 CH_3 of V18 of the Aβ16-28 peptide could have a small NOE interaction with either the Hδ2 P2 or the sugar protons (H37/H26) in the ligand giving evidence of an interaction between the two molecules (Figure 24).

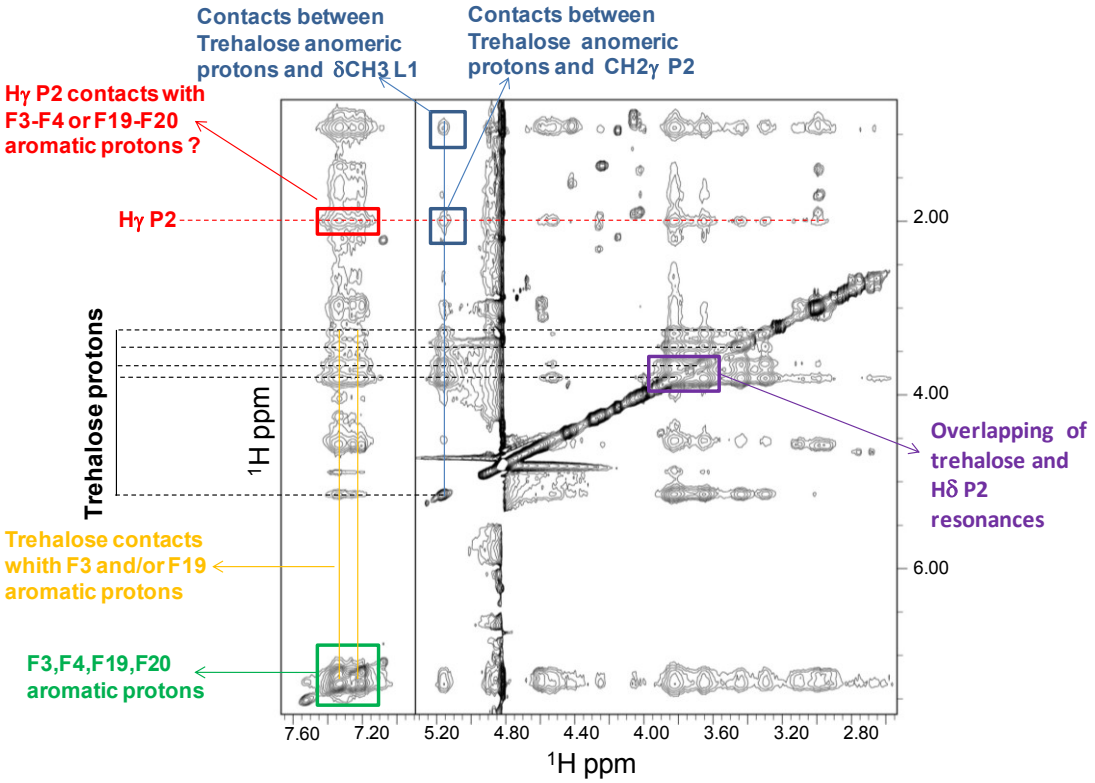

Figure 24. Expansion of a region from 2D [^{1}H, ^{1}H] NOESY of the complex Ac-LPFFD-Th 1 mM and Aβ16-28 1mM, in phosphate buffer at 27°C.

Evaluating the CSD from random coil values of Aβ16-28 in presence of the Ac-LPFFD-Th peptide (ratio 1:1), we can clearly see that the residue E22 has chemical shifts movements with respect to the Aβ16-28 alone (figure 25). This means that E22 could be involved in the recognition process. There are not great differences so it is possible that the main structural organization of the Aβ16-28 peptide should not be changed after binding to Ac-LPFFD-Th. However, several intra-molecular NOEs disappear (with respect to those observed in the unbound form, figure 23) due to line broadening.

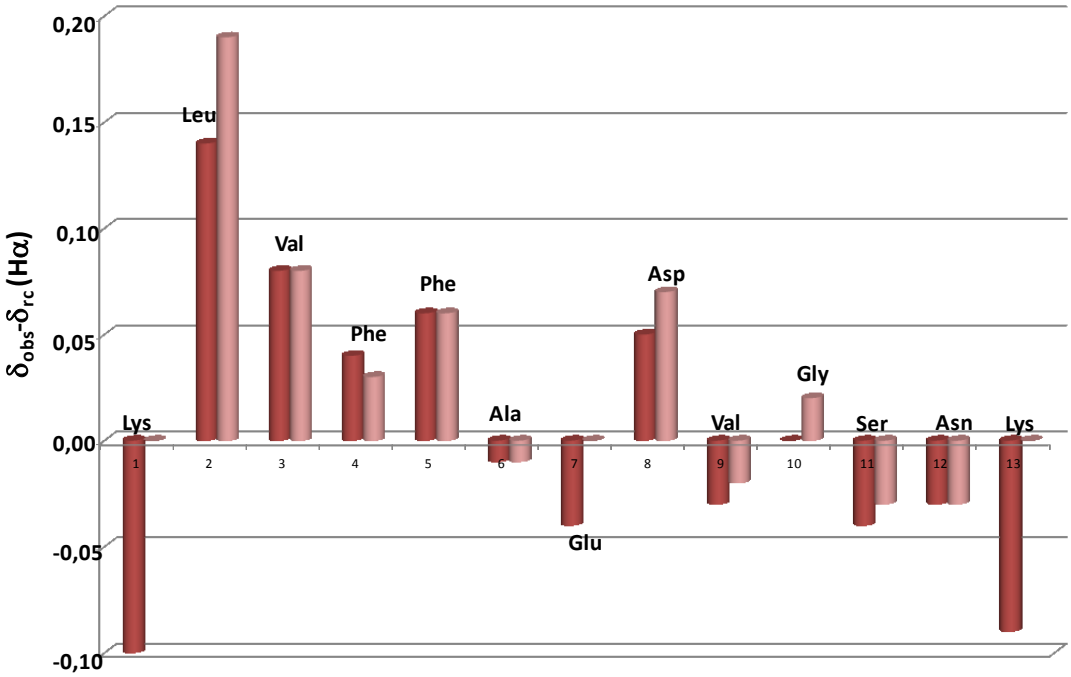

Figure 25. Comparison between CSD for Aβ16-28 Hα protons in presence (1:1 ratio) (pink) or in absence (red) of Ac-LPFFD-Th peptide. In the bound peptide we exclude Lys residues from the analysis since their Hα could not be unambiguously assigned.

Furthermore, other NMR studies of Ac-LPFFD-Th in presence of Aβ1-40 have been performed. The 1D [^{1}H] NMR spectrum of Ac-LPFFD-Th recorded at 600 μM concentration also shows sharp signals diagnostic of absence of aggregation processes (Figure 26 A). After addition of Aβ1−40 at a concentration equal to 250 or 30 μM, chemical shifts of Ac-LPFFD-Th do not undergo changes (Figure 26).

Interaction between Ac-LPFFD-Th and Aβ1−40 is evident in the NMR spectra recorded with the samples containing the amyloid at higher concentration (i.e. 250 μM). The 1D [^{1}H] spectrum of the Ac-LPFFD-Th/Aβ1−40 (molar ratio 2.4:1) complex is dominated by high intensity signals of the β-breaker peptide and low intensity lines of Aβ1-40 (figure 26 B) that likely belongs to residual monomeric species; in fact, according to previous studies signals from Aβ1−40 aggregated forms are NMR invisible. (84)

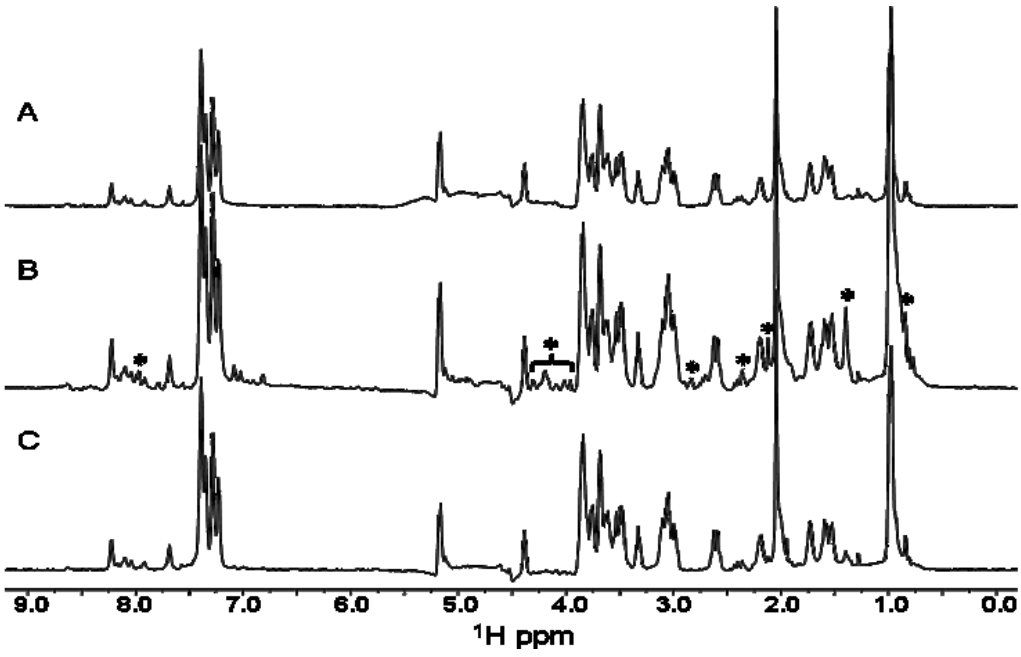

Figure 26. A) 1D Ac-LPFFD-Th 600 μM in 600 μL of phosphate buffer.
B) 1D Ac-LPFFD-Th 600 μM + 250 μM Aβ1-40 in 600 μL of phosphate buffer (ratio 2.4:1)
C) 1D Ac-LPFFD-Th 600 μM + 30 μM Aβ1-40 in 600 μL of phosphate buffer (ratio 20:1) * Aβ1-40 signals.

The 2D NOESY spectrum of the Ac-LPFFD-Th Apo-peptide contains almost exclusively diagonal peaks and highlights the flexibility of the small peptide; after addition of Aβ1–40 (in 2.4 fold defect) (figure 27), the increase of molecular weight upon complex formation, brings to the appearance of several negative NOEs, these NOEs are mainly intra-molecular contacts belonging to the Ac-LPFFD-Th peptide, we cannot see inter-molecular NOEs between Ac-LPFFD-Th and Aβ1–40 while we can observe only a few low intensity intra-molecular NOEs regarding Aβ1–40. In the complex, the proline in the β-breaker peptide is clearly in the trans configuration.

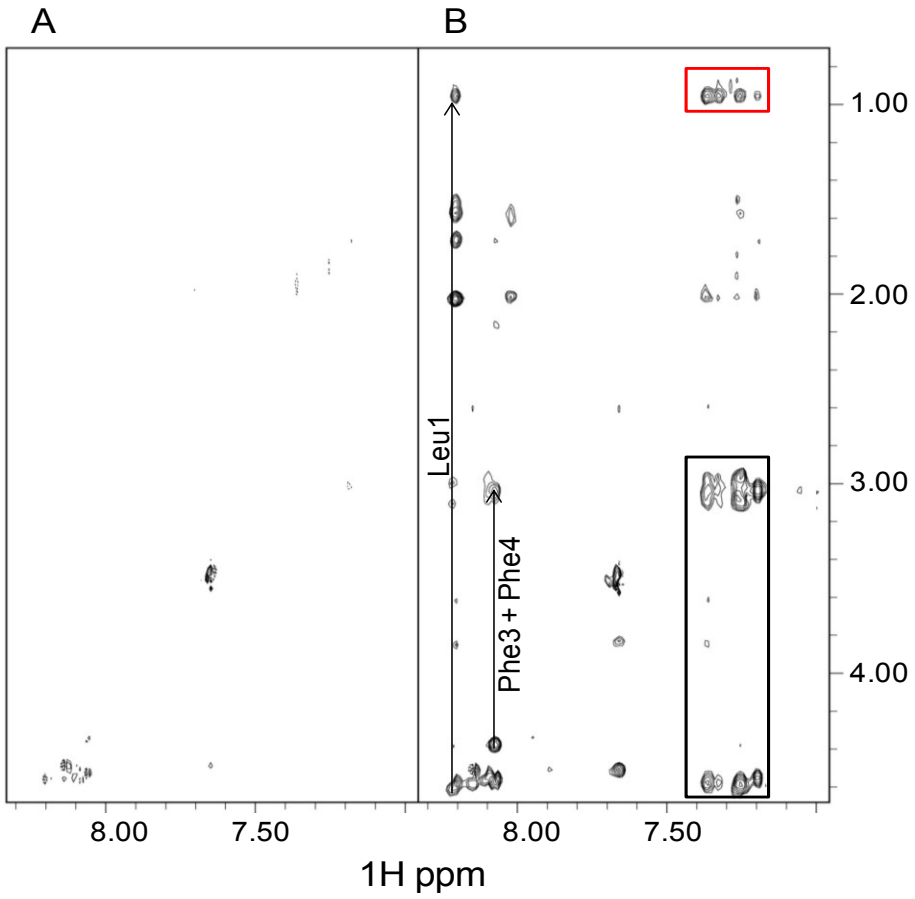

Figure 27. 2D [^{1}H, ^{1}H] NOESY spectra of Ac-LPFFD-Th peptide (600 µM concentration) alone (A) and after addition of Aβ1-40 (250 µM concentration). Intra-residue cross-peaks arising from aromatic protons of Phe3 and 4 and inter-residues noes between aromatic protons and Leu1 methyl groups in Ac-LPFFD-Th peptide are indicated by the black and red rectangles respectively (panel B).

We have recorded STD experiments as well and even if we were unable to get very high sensitivity and a complete binding epitope, it is evident that Leucine 1 methyl protons are contributing to the interaction with amyloid fibers (figure 28). We could not obtain by NMR any clear proof of direct interaction between the β-breaker peptide and Aβ1–40 monomer by using a "20 to 1" molar ratio.

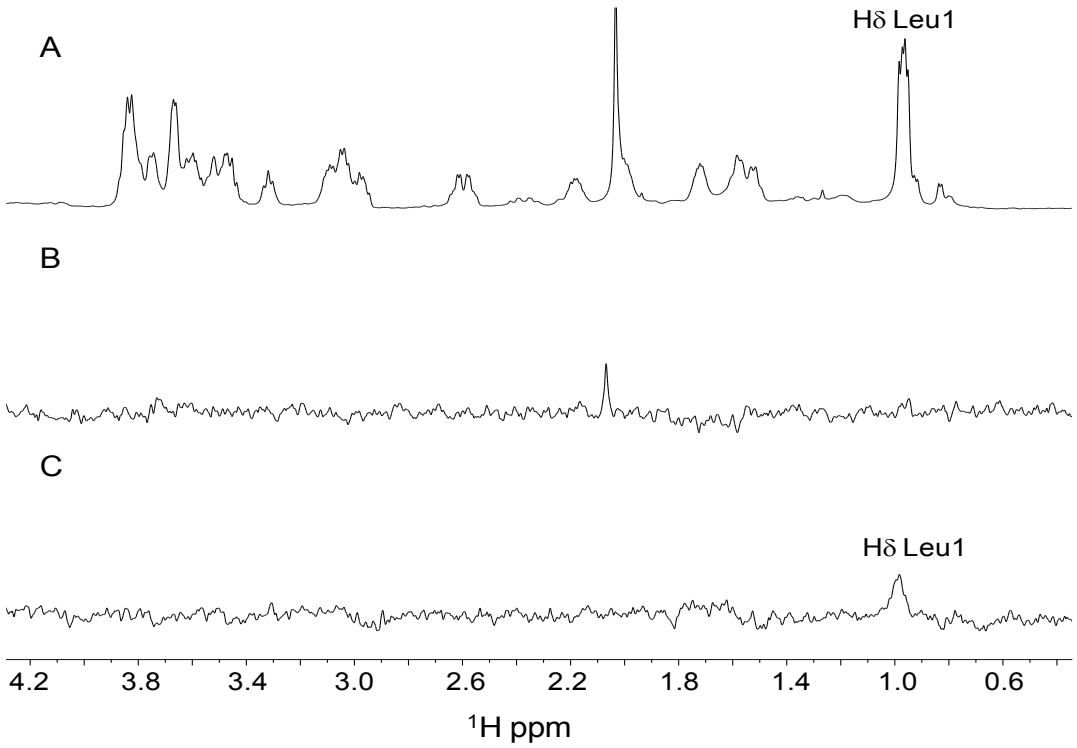

Figure 28. 1D [^{1}H] NMR spectrum of Ac-LPFFD-Th peptide (600 μM concentration, upper panel); STD reference spectrum of LPFFD-Th peptide (middle panel); STD spectrum of Ac-LPFFD-Th (600 μM concentration) plus Aβ1-40 (250 μM concentration).

3.5 Aß/AßOs WESTERN BLOT analysis

Previous studies demonstrated the formation of small soluble oligomeric assemblies derived from Aβ1-42 incubated in cell culture medium where the oligomeric assemblies were referred to as ADDLs (amyloid-derived diffusible ligands). (85)

For the studies presented herein, the cell culture medium method, with a 48-h incubation at 4 °C, was used to evaluate the nature and the amount of ADDLs formed by Aβ1-42 when co-incubated with Ac-LPFFD-Th. Western blot analysis of SDS-PAGE revealed that the incubated Aβ1-42 samples contained mostly high molecular weight oligomeric assemblies (50KDa) although tetramers, trimers, and monomers were also clearly detected (figure 29 *lane 1*). However the addition of Ac-LPFFD-Th during the incubation time corresponded to a marked increase in the amount of small Aβ1-42 forms (tetramers, trimers and monomers), while the smear corresponding to high molecular weight oligomeric assemblies almost disappeared. This unambiguously demonstrate that Ac-LPFFD-Th interfere with the formation of Aβ1-42 high molecular weight oligomeric assemblies.

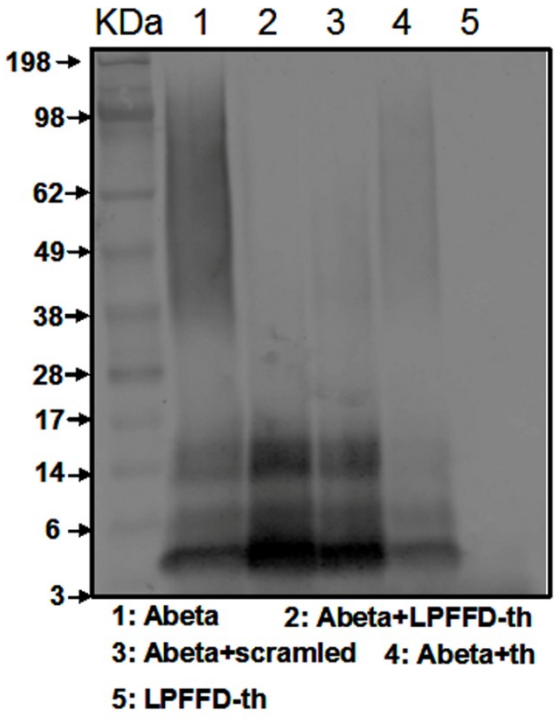

Figure 29. Representative Western blot of Aß1-42 oligomers produced upon incubation in presence or absence of Ac-LPFFD-Th or its respective control peptides, Samples were separated on a 4-12% bis-Tris gel SDS-PAGE, and visualised with the monoclonal antibody 6E10 (recognizing residues 1–16 of Aß). The representative figure shows that Aß1-42 give rise to high molecular weight oligomeric species (lane1) which disappear following the incubation with Ac-LPFFD-th (lane 2).

3.6 Neuroprotective activity of the beta sheet breaker-peptides

According to the aim of this work, a number of different biological experiments were performed to test the neuroprotective activity of the β-sheet-breaker peptide Ac-LPFFD-Th.

It is already known that toxicity of Aβ1-42 is confined to the oligomeric forms of the peptide and several publications have reported that monomers may have a role in neuronal metabolism. (86, 87, 88) It has also been shown that Aβ1-42 monomers are able to support the neuronal survival under conditions of tropic deprivation by acting on the PI-3-K pathway, that requires the activation of IGF-1/insulin receptor. Aβ1-42 monomers can protect mature cortical neurons against excitotoxicity death. (89)

In this regard, the inhibition of Aβ aggregation by the use of short peptides possessing beta sheet breaker activity, could provide an useful approach to prevent the formation of toxic oligomeric species and maintain the peptide in its physiologically active, monomeric form.

First of all we tested the neuroprotective activity of the Ac-LPFFD-Th peptide in comparison to the Soto peptide Ac-LPFFD-NH_2. We used two different Aβ-independent toxicity models: an excitotoxic model of NMDA insult performed on mixed cortical cultures (Figure 30) and pure cortical neurons maintained in an insulin deprived medium (Figure 31).

The results indicate that both peptides are neuroprotective at 100 nM on mixed neuronal cultures exposed to 300 μM NMDA for 10 min at room temperature in HEPES-buffered salt solution (Figure 30).

Trehalose alone was still able to decrease toxicity NMDA-mediated, however, if the peptides and trehalose share the same mechanism of neuroprotection is not clarified yet.

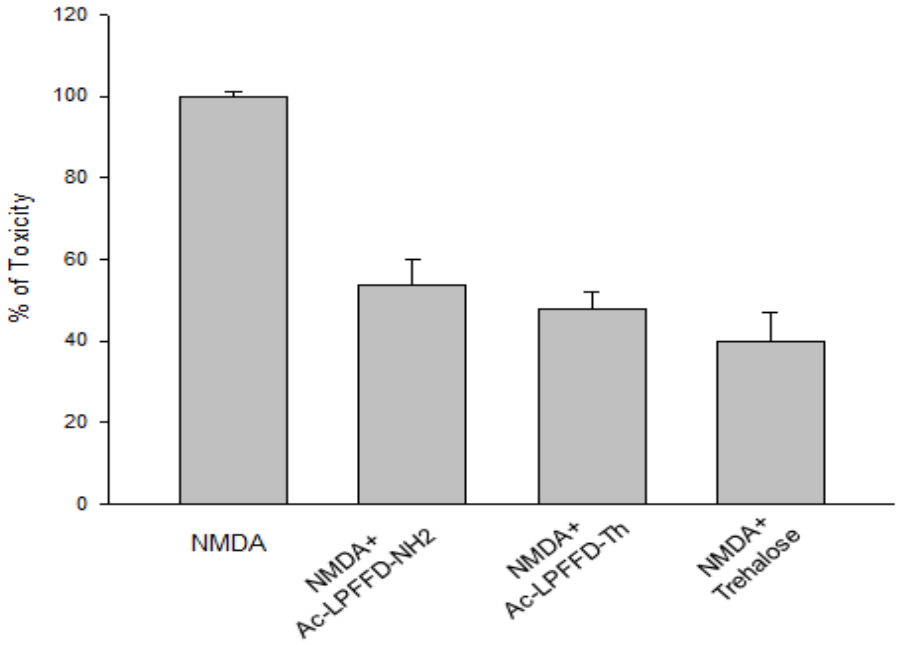

Figure 30. Excitotoxic model of NMDA insult performed on mixed cortical cultures. Ac-LPFFD-Th, Ac-LPFFD-NH2 and Trehalose all at 100nM concentration, on mixed neuronal cultures exposed to 300 μM NMDA for 10 min at room temperature in HEPES-buffered salt solution.

In Figure 31 the ability of Ac-LPFFD-NH_2 and Ac-LPFFD-Th (100 nM) to support neuronal survival in a trophic deprivation model is represented. During this experiment, pure neuronal culture were exposed to both the peptides in the absence of insulin support and maintained for 48 h at 37°C in 5% CO_2.

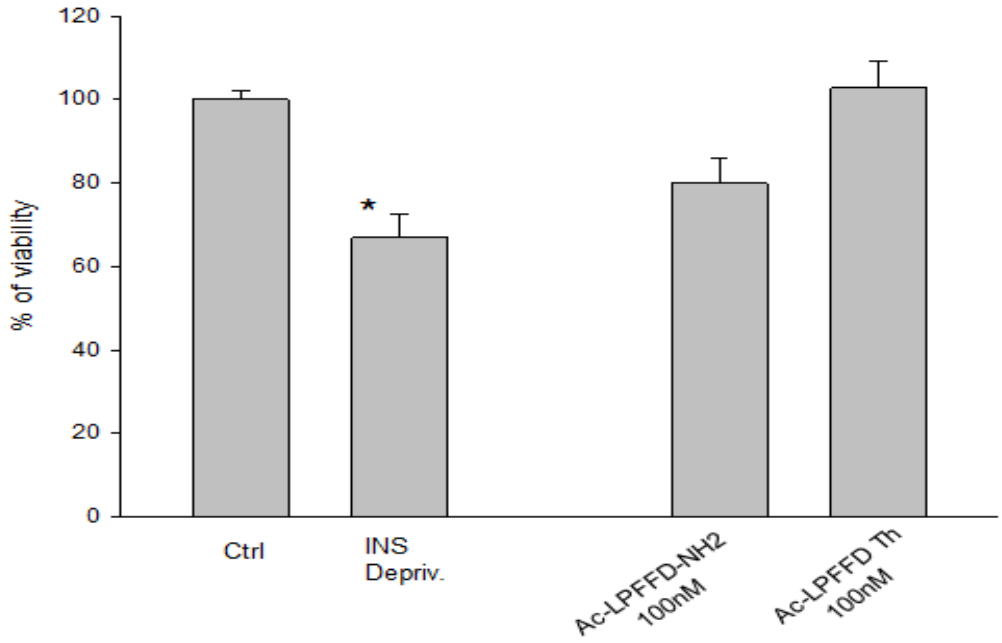

Figure 31. Neuronal survival in a trophic deprivation model. Ac-LPFFD-NH_2 and Ac-LPFFD-Th both at 100nM concentration. Pure neuronal culture were exposed to both the peptides in absence of insulin support and maintained for 48 h at 37°C in 5% CO_2.

The results show that Ac-LPFFD-NH_2 and Ac-LPFFD-Th are able to rescue cells viability. The presence of the trehalose mojety increases the neurotrophic activity of the Soto's peptide.

These data clearly indicate that the β-sheet-breaker peptides are " *per se*" neuroprotective as shown from both the experiments of excitotoxicity induced by NMDA and insulin depletion.

Furthermore in order to evaluate whether the Ac-LPFFD-NH_2 and Ac-LPFFD-Th derivatives, were able to prevent Aβ oligomers toxicity, a preparation of un-aggregated form of Aβ1-42 was incubated in the presence or absence of either Ac-LPFFD-NH_2 or Ac-LPFFD-Th at a final concentration of 100 µM (1:1 w/w, 48h at 4°C). Primary cortical neurons were treated with incubated Aβ1-42 samples diluted to 100 nM, for 2 days. This concentration produced a 40% of neuronal death as assessed by MTT assay. The co-incubation of Aβ1-42 with Ac-LPFFD-NH_2 prevented oligomers toxicity as shown in figure 32.

Notably, treatments with Ac-LPFFD-Th, produced a lack of toxicity, suggesting that trehalose conjugation, significantly increased the ability of the LPFFD pentapeptide to interfere with the formation of large oligomers which are responsible of neuronal death.

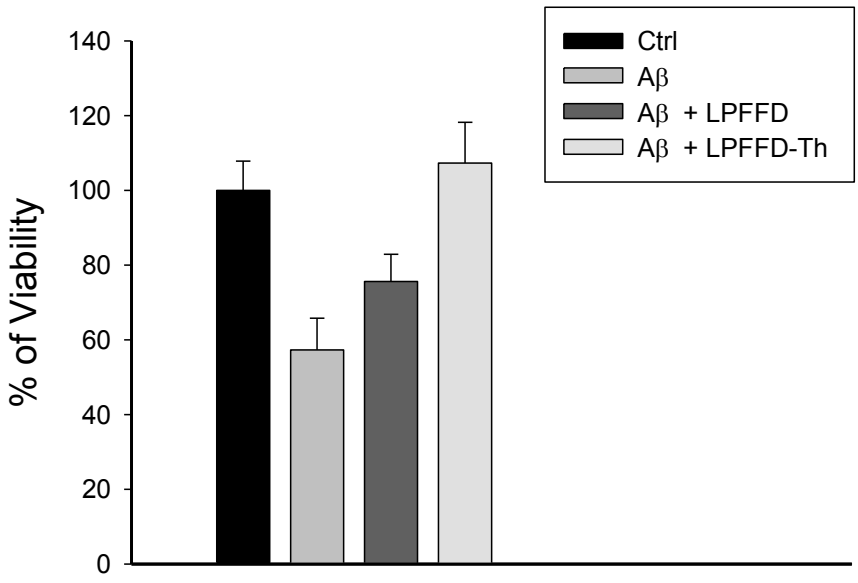

Figure 32. Cell viability was measured by MTT assay. Pure neuronal cultures were treated with pre-incubated samples of Aβ1-42 alone or in the presence of Ac-LPFFD-NH_2/Ac-LPFFD-Th,. The pentapeptides were added in a 5-fold molar excess with respect to Aβ1-42 for 48h at 4°C in DMEM-F12 . Values are the means ± SD of three independent experiments (n=3).

3.7 *In Vivo* study, Y-maze assay

To test the efficacy of Ac-LPFFD-Th *in vivo* model, the two-trial task in the Y-maze assay were performed as described in material and methods. The experiments were carried out at the Institut des Maladies Neurodégénératives, Université de Bordeaux, in collaboration with Dr. Oliver Nicole.

The Y-maze task is a specific and sensitive test of spatial recognition memory in rodents. The test relies on an innate tendency of rats to explore a novel environment. The Y-maze used in this study involves no aversive stimuli and was considered suitable for evaluating memory. (77)

Training was composed of the exploration (encoding) phase and the recognition phase, which were separated by various inter-trial intervals (ITIs). Memory performance was expressed as the percentage of time spent in novel arm ((seconds in novel arm)/(seconds in previously visited arms + seconds in novel arm) x 100).

In Figure 33 is shown how silencing of hippocampal activity with lidocaine infused after encoding impairs recognition memory probed 4 hours later compared to mice injected with vehicle (aCSF)(t_8=3.30; *p<0.05) (Figure 34, Right graph). Preliminary experiments (n=4/group) show that recognition memory in Aβ treated mice was impaired. This effect could be partially blocked by co-incubation with Ac-LPFFD-Th. These results should be validated by increasing the animal number.

Accordingly with this trial the Aβ1-42 treated rats exhibited the following: decrease of spontaneous alternations percentage within Y-maze task but in rat treated with Aβ1-42 co-incubated with the Ac-LPFFD-Th, we observed improved memory performance. (Figure 33, Right graph)

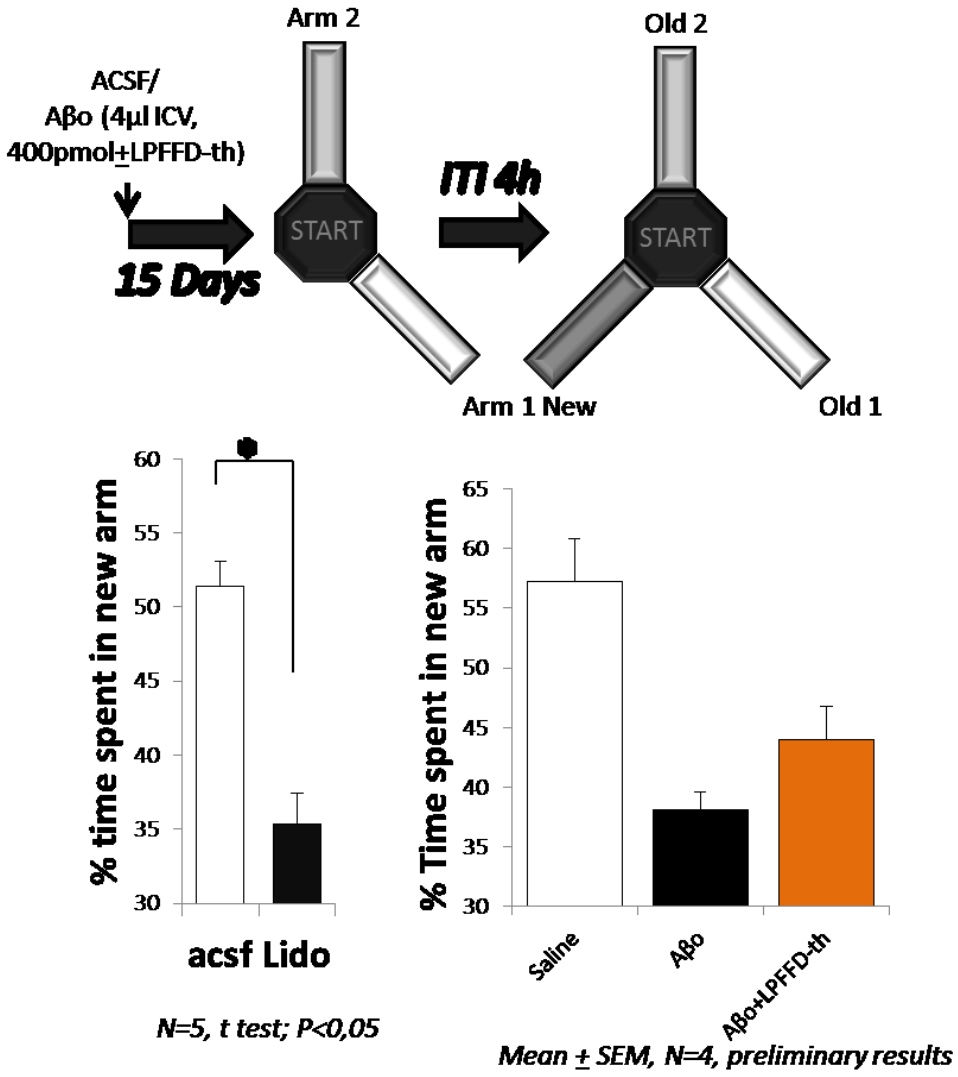

Figure: 33 (Left graph): Silencing of hippocampal activity with lidocaine infused after encoding impairs recognition memory probed 4 hours later compared to mice injected with vehicle (aCSF)(t_8=3.30; *p<0.05). (Right graph) Preliminary experiments (n=4/group) show that recognition memory in Aβ mice was impaired when probed 4 hours later and this effect could be partially block by co-incubation with Ac-LPFFD-Th. These results should be confirmed by increasing the animal number.

4. DISCUSSION

There is general agreement that monomeric Aβ is not toxic, but it becomes toxic to neuronal cells once it is aggregated.(89,90) Since Aβ's soluble self-assembled forms (i.e oligomers and protofibrils) are believed to act as the actual toxic entities to cultured cells, an intervention at the very early stages of Aβ1-42 aggregation may represent a valid approach to prevent neuronal degeneration. However, in depth molecular studies of soluble oligomers are difficult to carry out because of the transient nature and instability of such aggregates. (91) As a consequence, the molecular mechanism underlying the action of the inhibitors of amyloid aggregation has not been clearly understood. In particular, it has to be established whether peptide-based inhibitors stabilize the Aβ monomer or target the Aβ aggregated forms. In this thesis it has been shown that Ac-LPFFD-Th is able to prevent the formation of both β-sheet rich aggregated and large oligomeric assemblies of Aβ1-42 as demonstrated by Th-T measurements and Western blot analysis respectively (see Figures 7,8,9,10 and Figure 29). As a matter of fact, distinct morphological species including oligomers, protofibrils and fibrils are formed during the aggregation process, and all these aggregation states are expected to co-exist, along with monomers, in the Aβ sample solution. Therefore, if taken alone each experiment carried out in the present study cannot give comprehensive information, of which molecular species of Aβ1-42 the peptide inhibitor is interacting with. Our ESI-MS results provide direct evidence of the existence of a molecular adduct between the Aβ1-42 monomer and Ac-LPFFD-Th. On the other hand we cannot rule out that the Ac-LPFFD-Th derivative could interact with Aβ1-42 aggregated forms. In this regard, we used NMR to detect binding between Ac-LPFFD-Th and Aβ aggregated forms and we were able to get proof of binding, through STD and NOESY experiments, at the higher concentration of Aβ1-40 (i.e., 250 μM) only. In these conditions the aggregation level of the amyloid peptide is relatively high and the type of NMR experiments, that we run, generally works when binding is weak (in the micromolar-millimolar range). At the lower concentration of Aβ1-40 (i.e., 30 μM), aggregation phenomena are less relevant and NMR fails to detect the interaction.

These results seem to confirm that Ac-LPFFD-Th can bind to aggregated forms of the amyloid peptide and are in nice agreement with other works related to the interaction between a sugar containing peptidomimetic molecule and Aβ1-40. (84) Considering recent computational studies, (92,93) it may be hypothesized that Ac-LPFFD-Th inhibitor can intercept low molecular weight (LMW) aggregated forms, thus preventing both toxic oligomer formation (i.e. dodecamers) and recruitment of Aβ monomers in fibril formation. Notably, such an hypothesis is consistent with the significant amount of Aβ1-42 monomer observed in the western blot analysis after 48 h incubation in the presence of Ac-LPFFD-Th (see Figure 29). Our assumption finds also support in the DLS measurements indicating that Aβ1-42 aggregation process does not evolve into species bigger than 10 nm when incubated in the presence of Ac-LPFFD-Th (see figure 13). The dose responsive antifibrillogenic activity is evident from the Th-T experiments. Here an almost complete flattening of the exponential phase, where elongation of protofibrils occurs, is observed at 20 fold molar excess of Ac-LPFFD-Th (See Figure 9). However Th-T can detect only β-sheet rich amyloid fibril and not monomers or oligomers, (94) thus on the basis of the Th-T fluorescence alone, the formation of neurotoxic aggregated forms cannot be excluded even in the presence of the peptide inhibitors. Despite numerous studies, controversy still exists as to whether oligomers that appear transiently at different stages during fibrillization are simply intermediates on the pathway leading to fibril formation, or whether they represent ‘‘off pathway’’ aggregates that populate alternative aggregation pathways. (95) In light of these considerations, inhibitors should be conceived as capable of blocking both entities, oligomers and fibrils, considered as potentially toxic. In fact if Aβ oligomers are simply intermediates on the pathway to fibril formation, then molecules that prevent oligomers formation would also be expected to prevent amyloid formation. However, if fibrils and oligomers represent distinct aggregation pathways, then some inhibitors might block Aβ oligomerization but not necessarily fiber formation or vice versa. According to the information obtained by western blot analysis, MTT assay showed that in absence of the peptide inhibitors, Aβ incubated for 48 hours at 4°C, was able to induce neuronal toxicity (about 40% of cell death) by virtue of the high molecular species promoted by the application of the Lambert protocol as revealed by electrophoresis gel (see Figure 29 lane 1).

Interestingly, and as expected, the presence of Ac-LPFFD-NH_2 during the time of Aβ incubation substantially decreased Aβ toxicity, confirming that this peptide may inhibit the auto-assembly of Aβ into high molecular weight species. In the same condition, the Ac-LPFFD-Th showed to be even more effective in preventing Aβ toxicity as demonstrated by the total rescue of neuronal death. Interestingly, western blot analysis of Aβ1-42 incubated with Ac-LPFFD-Th significantly differs from the one with Aβ alone. The incubation of Aβ1-42 in DMEM-F12 for 48 hours at 4°C promotes the formation of soluble oligomeric species ranging approximately from 38 to 100 kDa which are known to differentially affect cell viability. The interaction of Ac-LPFFD-Th with Aβ1-42 prevents the formation of aggregates with size higher than 17kDa, while the band corresponding to monomeric form of Aβ (4 kDa) is clearly increased. Based on these data, the underlying mechanism by which this peptide prevents the neurotoxicity of Aβ1-42 oligomers seems to lie on the ability to interfere with the generation of high molecular weight oligomers. This in turn will increase the amount of less toxic and/or non toxic species, such as the monomeric form of Aβ1-42 recently reported to have a broad range of physiological activity including the ability to activate survival pathway. (89) Our results are once more in nice agreement with other Authors who found that stabilizing monomers or small oligomers ($8 \leq RH \leq 12$ nm) drastically reduced cell toxicity of Aβ preparations. (96)

The Ac-LPFFD-Th β-sheet breaker peptide is also neuroprotective "*per se*" and this is demonstrated by experiments of excitotoxicity induced by NMDA and insulin depletion (figure 30 and 31 respectively).

Even more important, our data show that Ac-LPFFD-Th is a potent inhibitor of Aβ fibrillation and this ability appears specifically directed against Aβ peptides.

In fact, the specificity of action of the Ac-LPFFD-Th peptide was demonstrated by our comparative Th-T experiments of fibril formation carried out using the human Islet Amyloid Polypeptide (hIAPP), another well known amyloidogenic peptide involved in type 2 diabetes mellitus. (79, 80) We found that hIAPP fibrillogenesis was accelerated in the presence of 5 and 20 fold molar excess of Ac-LPFFD-Th (figure 11). In agreement with other studies, co-polymerization might occur when hIAPP and Ac-LPFFD-Th are incubated together and this leads to the enhancement of amyloid formation. (84,97)

Surprisingly, at the micromolar concentrations we used, trehalose was neuroprotective despite it did not exhibit significant antifibrillogenic activity in the Th-T fluorescence assay (figure 9).

Actually, trehalose has been found to be effective in the treatment of neurodegenerative diseases associated with peptide or protein aggregation, but at the millimolar concentration that are at least three orders of magnitude higher than the micromolar concentrations used in the present study. Trehalose has been also indicated as an activator of autophagy and increased autophagy has been found to reduce Aβ levels and improve cognitive function in a mouse model of AD. (98,99) We are aware that further work is required to elucidate the precise role of the trehalose moiety in the neuroprotection observed in our experiments. Our previous results indicated that trehalose endows the LPFFD peptide with enhanced stability in biological fluids. (70) Therefore, we can speculate that retardation of Aβ fibril formation in combination with enhanced clearance of Aβ aggregated states, due to activation of neuronal autophagy, are two concurrent mechanisms that might explain the neuroprotective activity observed in the primary neuronal cell cultures.

Furthermore, we investigated the effects of our BSB peptide on cognitive function in mice treated with Aβo in presence or absence of Ac-LPFFD-Th, using the Y-maze task. We demonstrated the following novel findings: treatment with Aβo induced cognitive impairment as expected, treatment with Ac-LPFFD-Th seems to block this memory impairment.

Conclusions

In this PhD thesis we provide evidences of a direct interaction between the β-sheet-breaker peptides Ac-LPFFD-Th and the Aβ peptide. The ability of our BSB to recognize and bind low molecular weight aggregated forms of Aβ has been investigated by means of different biophysical techniques, including Th-T fluorescence, DLS, ESI-MS and NMR. Moreover, biological assays on murine cortical primary neuronal cultures were carried out in order to clarify and further characterize the mechanism of cytoprotection exhibited by the Ac-LPFFD-Th.

In addition we have shown that the treatment with Aβo induces cognitive impairment as expected, whereas the treatment with Ac-LPFFD-Th seems to block this memory impairment due to Aβo.

Further work is required to elucidate the role of the trehalose moiety in the neuroprotection observed in our experiments.

References

1) C. M. Dobson, Protein Misfolding, Aggregation, and Conformational Diseases, *Protein Reviews*, 2006, 4, 21-41.

2) K. Diederichs and A. Karplus, *Nature Structural Biology*, 1997, 4, 269 – 275

3) C.M. Dobson, Protein folding and misfolding, *Nature*, 2003, 426, 884-90.

4) K.A. Dill, H.S. Chan, From Levinthal to pathways to funnels, *Nature Structural Biology*, 1997, 4, 10-19.

5a) M. Calamai, F. Chiti, C.M. Dobson, Amyloid fibril formation can proceed from different conformations of a partially unfolded protein, *Biophys J*. 2005, 89, 4201-10.

5b) H.J. Dyson, P.E. Wright, H.A. Scheraga, The role of hydrophobic interactions in initiation and propagation of protein folding, *PNAS*, 2006, 103, 35.

6) B. Hardesty, G. Kramer, Folding of a nascent peptide on the ribosome, *Prog Nucleic Acid Res Mol Biol*. 2001, 66, 41-66.

7) B. Bösl, V. Grimminger, S. Walter, The molecular chaperone Hsp104, a molecular machine for protein disaggregation. *J Struct Biol*. 2006, 156, 139-48.

8) L.C. Serpell, M. Sunde, C.C. Blake, The molecular basis of amyloidoses, *Cell Mol Life Sci*. 1997, 53, 871-87.

9) V. N. Uversky, A. Fernández, A. L. Fink. Structural and Conformational Prerequisites of Amyloidogenesis, *Protein Reviews*, 2006, 4, 1-20.

10) P.G Ridge, M.T Ebbert, J.S. Kauwe, Genetics of Alzheimer's disease, *Biomed. Res. Int.* 2013, 254954.

11) M. Sathya, P. Premkumar, C. Karthick, P. Moorthi, K.S. Jayachandran, M. Anusuyadevi, BACE1 in Alzheimer's disease, *Clin Chim Acta*. 2012, 414, 171-8.

12) A.D. Hardy, G.A. Higgins, Alzheimer's disease: the amyloid cascade hypothesis, Science, 1992, 256, 184.

13) B.D. Strooper, T. Iwatsubo, M.S. Wolfe. Presenilins and γ-Secretase: Structure, Function, and Role in Alzheimer Disease. *Cold Spring Harb Perspect Med*, 2012, 2.

14) P. Cizas, R. Budvytyte, R. Morkuniene, R. Moldovan, M. Broccio, M. Lösche, G. Niaura, G. Valincius, V. Borutaite, Size-dependent neurotoxicity of beta-amyloid oligomers, *Arch Biochem Biophys*. 2010, 496, 84-92.

15) M.S. Parihar, G.J. Brewer Amyloid-β as a Modulator of Synaptic Plasticity *J Alzheimers Dis*. 2010, 22, 741-763.

16) G.M. Bishop, S.R. Robinson, The amyloid paradox: amyloid-beta-metal complexes can be neurotoxic and neuroprotective, Brain Pathol. 2004, 14 ,4, 448-52.

17) K. Zou, J.S. Gong, K. Yanagisawa, M. Michikawa, A novel function of monomeric amyloid beta-protein serving as an antioxidant molecule against metal-induced oxidative damage. *J. Neurosci.* 2002, 22, 12, 4833-41.

18) M.L. Giuffrida, A. Copani et all. Beta-amyloid monomers are neuroprotective, *J Neurosci*. 2009, 29, 34, 10582-7.

19) F.L. Heppner, R.M. Ransohoff, B. Becher. Immune attack: the role of inflammation in Alzheimer disease, *Nat Rev Neurosci*. 2015, 16, 6, 358-72.

20) M.A. Meraz-Ríos, V. Campos-Peña et al, Inflammatory process in Alzheimer's Disease**,** *Front. Integr. Neurosci.* 2013, 13.

21a) K.J. Korshavn, A. Bhunia, M.H. Lim, A. Ramamoorthy, Amyloid-β adopts a conserved, partially folded structure upon binding to zwitterionic lipid bilayers prior to amyloid formation, *Chem Commun,* 2015.

21b) Terzi, E., Holzemann, G. and Seelig, J Interaction of Alzheimer bamyloid peptide(1–40) with lipid membranes, Biochemistry, 2007, 36, 14845– 14852.

22) Z. Dong, P. Saikumar, J.M. Weinberg, M.A. Venkatachalam, Calcium in cell injury and death, *Annu. Rev. Pathol. Mech*. 2006, 1, 405–434.

23) a) X. Yu, J. Zheng, Cholesterol promotes the interaction of Alzheimer b-amyloid monomer with lipid bilayer, *J. Mol. Biol*. 2012, 421, 561–571. b) R. Liu, T. Tian, J. Jia, Characterization of the interactions between b-amyloid peptide and the membranes of human SK-N-SH cells, *FEBS Letters*, 2015, 589, 1929–1934.

24) F.J. Sepulveda, L.G. Aguayo, Synaptotoxicity of Alzheimer Beta Amyloid Can Be Explained by Its Membrane Perforating Property, *PLoS One,* 2010, 5, 7, 11820.

25) I.C. Martins, F. Rousseau et al. Lipids revert inert Aβ amyloid fibrils to neurotoxic protofibrils that affect learning in mice. *EMBO J*. 2008, 27, 1, 224–233.

26) K. Broersen, F. Rousseau, J. Schymkowitz, The culprit behind amyloid beta peptide related neurotoxicity in Alzheimer's disease: oligomer size or conformation? *Alzheimers Res Ther*. 2010, 2, 12.

27) A. Abedini, D.P. Raleigh, Protein Engineering, *Design & Selection* 2008, 22 453–459.

28) W. Hoyer, C. Grönwall, A. Jonsson, S. Ståhl, T. Härd, Stabilization of a β-hairpin in monomeric Alzheimer's amyloid-β peptide inhibits amyloid formation, *PNAS*, 2008, 105, 5099–5104.

29) V. N. Uversky, Mysterious oligomerization of the amyloidogenic proteins, *FEBS J*. 2010 277, 2940–2953.

30) K. Brännström, A. Öhman, A. Olofsson, Aβ Peptide Fibrillar Architectures Controlled by Conformational Constraints of the Monomer, PLoS One, 2011, 6,9, e25157.

31) W. Kim, M.H. Hecht, J Biological Chemistry, 2005, 280, 41, 35069–35076.

32) M.M. Murray, S.L. Bernstein, V, Nyugen, M.M. Condron, D.B. Teplow, M.T. Bowers, Amyloid β-protein: Aβ1-40 Inhibits Aβ1-42 Oligomerization, *J Am Chem Soc*. 2009, 131, 18, 6316–6317.

33) A. Jan, O. Gokce, R. Luthi-Carter, H.A. Lashuel, The Ratio of Monomeric to Aggregated Forms of Aβ1-40 and Aβ1-42 Is an Important Determinant of Amyloid-β Aggregation, Fibrillogenesis, and Toxicity, J Biol Chem. 2008, 283, 42, 28176–28189.

34) I. W. Hamley. The Amyloid Beta Peptide: A Chemist's Perspective. Role in Alzheimer's and Fibrillization. *Chem. Rev*. 2012, 112, 5147−5192.

35) J.S. Jacobsen, F.E. Bloom, et al, Early-onset behavioral and synaptic deficits in a mouse model of Alzheimer's disease. Proc Natl Acad Sci U S A, 2006. 103, 5161-6.

36) T.A. Lanz, D.B. Carter, K.M. Merchant, Dendritic spine loss in the hippocampus of young PDAPP and Tg2576 mice and its prevention by the ApoE2 genotype, Neurobiol Dis. 2003, 13, 246-53.

37) Y.M. Kuo , M.R. Emmerling MR, C. Vigo-Pelfre, T.C Kasunic, et al. Water-soluble Abeta (N-40, N-42) oligomers in normal and Alzheimer disease brains. *J Biol Chem*. 1996, 271, 4077-81.

38) R. Kayed , E. Head, et al. Common structure of soluble amyloid oligomers implies common mechanism of pathogenesis. *Science*. 2003, 300, 486-9.

39) Y. Gong, L. Chang, et al Alzheimer's disease-affected brain: presence of oligomeric A beta ligands (ADDLs) suggests a molecular basis for reversible memory loss. *Proc Natl Acad Sci U S A*. 2003, 100, 10417-22.

40) P.N Lacor, M.C. Buniel, Synaptic targeting by Alzheimer's-related amyloid beta oligomers.,. *J Neurosci*. 2004, 24, 10191-200.

41) L.F Lue, K.M Kuo, Soluble amyloid beta peptide concentration as a predictor of synaptic change in Alzheimer's disease. *J Am J Pathol*. 1999, 155, 853-62.

42) L. Mucke, G.Q Yu, et al, .Astroglial expression of human alpha(1)-antichymotrypsin enhances alzheimer-like pathology in amyloid protein precursor transgenic mice. *Am J Pathol*. 2000, 157, 2003-10.

43) D.L Moolman, O.V. Vitolo, Dendrite and dendritic spine alterations in Alzheimer models. *J Neurocytol*. 2004, 33, 377-87.

44) J.R. Steinerman, et al, Distinct pools of beta-amyloid in Alzheimer disease-affected brain: a clinicopathologic study. *Arch. Neurol*. 2008, 65, 906-12.

45) M. Menéndez-González, J.A. Vega, Immunotherapy for Alzheimer's disease: rational basis in ongoing clinical trials. *Curr Pharm Des.* 2011, 17, 5, 508-20.

46) M. Menéndez-González, J.A. Vega, Immunotherapy for Alzheimer's disease: rational basis in ongoing clinical trials. *Curr Pharm Des.* 2011, 17, 5, 508-20.

47) B.D. Strooper, T. Iwatsubo, M.S. Wolfe, Presenilins and γ-Secretase: Structure, Function, and Role in Alzheimer Disease. *Cold Spring Harb Perspect Med*, 2012, 2.

48) R. Yan, R.Vassar, Targeting the β secretase BACE1 for Alzheimers disease therapy, *Lancet Neurology*, 2014, 13, 3, 319-329.

49) R. Vassar, P.C. Kandalepas, The β-secretase enzyme BACE1 as a therapeutic target for Alzheimer's disease., *Alzheimer's Research & Therapy.* 2011, 3, 20.

50) M. Cruz, et al, Inhibition of beta-amyloid toxicity by short peptides containing N-methyl amino acids, J Pept Res. 2004, 63, 3, 324-8.

51) A.D Ferrão-Gonzales, et al, Controlling {beta}-amyloid oligomerization by the use of naphthalene sulfonates: trapping low molecular weight oligomeric species, *J Biol Chem.* 2005, 280, 41, 34747-54.

52) A.J. Doig, et al, Inhibition of toxicity and protofibril formation in the amyloid-beta peptide beta(25-35) using N-methylated derivatives, *Biochem Soc Trans*. 2002, 30, 4, 537-42.

53) K. Wiesehan, Selection of D-amino-acid peptides that bind to Alzheimer's disease amyloid peptide abeta1-42 by mirror image phage display, *Chembiochem*, 2003, 4, 8, 748-53.

54) G. Forloni, M. Salmona, et al, Anti-amyloidogenic activity of tetracyclines: studies in vitro. FEBS Lett. 2001, 487, 3, 404-7.

55) L. Diomede, M. Salmona, et al, Tetracycline and its analogues protect Caenorhabditis elegans from β amyloid-induced toxicity by targeting oligomers, *Neurobiol Dis*. 2010, 40, 2, 424-31

56) B. Matharu, B, Austen, et al, Galantamine inhibits beta-amyloid aggregation and cytotoxicity, J Neurol Sci. 2009, 280, 1, 49-58.

57) A.R. Ladiwala, P.M. Tessier, et al, Resveratrol selectively remodels soluble oligomers and fibrils of amyloid Abeta into off-pathway conformers, J Biol Chem. 2010, 285, 31, 24228-37.

58) A. Srinivasan, Experimental Inhibition of Peptide Fibrillogenesis by Synthetic Peptides, Carbohydrates and Drugs, *Springer,* 2012, 12, 271-294.

59) F.F. Liu, L. Ji, X.Y. Dong, Y. Sun, Molecular insight into the inhibition effect of trehalose on the nucleation and elongation of amyloid beta-peptide oligomers. *J Phys Chem B*. 2009, 113, 32, 11320-9.

60) J.D. Andya , C.C. Hsu, S.J. Shire, Mechanisms of aggregate formation and carbohydrate excipient stabilization of lyophilized humanized monoclonal antibody formulations, *AAPS PharmSci.* 2003, 5, 2, E10.

61) J. Ryu, C.B Park, Inhibition of beta-amyloid peptide aggregation and neurotoxicity by alpha-d-mannosylglycerate, a natural extremolyte, *Peptides*, 2008, 29, 4, 578-84.

62) U. Das, A. Srinivasan, et al, Interface peptide of Alzheimer's amyloid beta: application in purification, *Biochem Biophys Res Commun*. 2007, 362, 2, 538-42.

63) M.M. Pallitto, R.M. Murphy, Recognition sequence design for peptidyl modulators of beta-amyloid aggregation and toxicity, *Biochemistry*, 1999, 38, 12, 3570-8.

64) D.J. Gordon, K.L. Sciarretta, S.C. Meredith, Inhibition of beta-amyloid(40) fibrillogenesis and disassembly of beta-amyloid(40) fibrils by short beta-amyloid congeners containing N-methyl amino acids at alternate residues, *Biochemistry*, 2001, 40, 28, 8237-45.

65) A. Kapurniotu, M Nossol, et al, Conformational restriction via cyclization in beta-amyloid peptide Abeta(1-28) leads to an inhibitor of Abeta(1-28) amyloidogenesis and cytotoxicity. *Chem Biol.* 2003, 10, 2, 149-59.

66) J.F. Poduslo, C. Soto, Beta-sheet breaker peptide inhibitor of Alzheimer's amyloidogenesis with increased blood-brain barrier permeability and resistance to proteolytic degradation in plasma, J Neurobiol. 1999, 39, 3, 371-82.
67) C. Soto, et al, Beta-sheet breaker peptides inhibit fibrillogenesis in a rat brain model of amyloidosis: implications for Alzheimer's therapy, *Nat Med*. 1998, 4, 7, 822-6.)

68) C. Adessi, C. Soto, et al, Pharmacological profiles of peptide drug candidates for the treatment of Alzheimer's disease, *J Biol Chem*. 2003, 278, 16, 13905-11.

69) T. Härd, C. Lendel, Inhibition of amyloid formation. *J. Mol Biol.* 2012, 421, 441-65.
70) P. De Bona, M.L Giuffrida, F. Caraci, A. Copani, B. Pignataro, F. Attanasio, S. Cataldo, G. Pappalardo, E, Rizzarelli, Design and synthesis of new trehalose-conjugated pentapeptides as inhibitors of Abeta(1-42) fibrillogenesis and toxicity. *J Pept Sci*. 2009, 15, 220-228.
71) F. Attanasio, C. Cascio, S. Fisichella, V.G. Nicoletti, B. Pignataro, A. Savarino, E. Rizzarelli, Trehalose effects on alpha-crystallin aggregates**,** *Biochem Biophys Res Commun.* 2007, 354, 4, 899-905.

72 T. Jiang, W.B. Yu, T. Yao, X.L. Zhi, L.F. Pan, J. Wang, P. Zhou, Trehalose inhibits fibrillation of A53T mutant alpha-synuclein and disaggregates existing fibrils. *RSC Adv.* 2013, 3, 9500−9508.

73) S. Sarkar, D.C. Rubinsztein, Small molecule enhancers of autophagy for neurodegenerative diseases, *Mol Biosyst*. 2008, 4, 8, 895-901.

74) M.L. Giuffrida, F. Caraci, P. De Bona, G. Pappalardo, F. Nicoletti, E. Rizzarelli, A. Copani, The monomer state of beta-amyloid: where the Alzheimer's disease protein meets physiology, *Rev. Neurosci.,* 2010, 21, 83-93.
75) A. Copani, F. Condorelli, A. Caruso, C. Vancheri, A. Sala, A.M. Giuffrida Stella, P.L. Canonico, F. Nicoletti, M.A. Sortino, *FASEB J.* 1999, 13, 15, 2225-34
76) V. Bruno, A. Copani, F. Nicoletti, et al, Activation of metabotropic glutamate receptors coupled to inositol phospholipid hydrolysis amplifies NMDA-induced neuronal degeneration in cultured cortical cells. Neuropharmacology, 1995, 34, 1089-98.

77) T. Maviel, B. Bontempi, et al, Sites of Neocortical Reorganization Critical for Remote Spatial Memory, *Science* 2004,305,96-99.

78) F. Dellu, H. Simon et al, Extension of a new two-trial memory task in the rat: influence of environmental context on recognition processes, *Neurobiol Learn Mem.* 1997, 67, 2, 112-20

79) M.F. Tomasello, A. Sinopoli, G. Pappalardo, On the environmental factors affecting the structural and cytotoxic properties of IAPP peptides. *Journal of Diabetes Research;* 2015 ID 918573.

80) M.F. Tomasello, A. Sinopoli, F. Attanasio, M.L. Giuffrida, T. Campagna, D. Milardi, G. Pappalardo, Molecular and cytotoxic properties of hIAPP17-29 and rIAPP17-29 fragments: A comparative study with the respective full-length parent polypeptides, *Eur. J. Med. Chem*. 2014, 81, 442–455.

81) M. Landreh, G. Alvelius, J. Johansson, H. Jörnvall, Insulin, islet amyloid polypeptide and C-peptide interactions evaluated by mass spectrometric analysis, *Rapid Communications in Mass Spectrometry*, 2014, 28, 2, 178–184.

82) M. Kjaergaard, S. Brander, F.M. Poulsen, Random coil chemical shift for intrinsically disordered proteins: effects of temperature and pH, *J Biomol NMR*, 2011, 49, 2, 139-149.

83) R. Riek, P. Güntert, H. Döbeli, B. Wipf, K. Wüthrich, NMR studies in aqueous solution fail to identify significant conformational differences between the monomeric forms of two Alzheimer peptides with widely different plaque-competence, $A\beta(1–40)^{ox}$ and $A\beta(1–42)^{ox}$, *European Journal of Biochemistry* 2001, 268, 22, 5930–5936.

84) B. Dorgeret, L. Khemtémourian, I. Correia, J.L. Soulier, O. Lequin, S. Ongeri, Sugar-based peptidomimetics inhibit amyloid β-peptide aggregation, *Eur J Med Chem.* 2011, 46, 12, 5959-5969.

85) M.P. Lambert, A. K. Barlow, M. Liosatos, G.A Krafft, W.L. Klein, *et al*. *Proc. Natl. Acad. Sci U. S. A.* 1998, 95, 6448–6453.

86) M.S. Parihar, G.J. Brewer, Amyloid-β as a modulator of synaptic plasticity. J. Alzheimers Dis. 2010, 22, 741-63.

87) G.M. Bishop, R.S. Robinson, The amyloid paradox: amyloid-beta-metal complexes can be neurotoxic and neuroprotective, *Brain Pathol*. 2004, 14, 448-52.

88) K. Zou, J.S. Gong, K. Yanagisawa, M. Michikawa, A novel function of monomeric amyloid beta-protein serving as an antioxidant molecule against metal-induced oxidative damage, *J. Neurosci.* 2002, 22, 4833-41.

89) M.L. Giuffrida, G. Pappalardo, E. Rizzarelli E, A. Copani, *et al.* Beta-amyloid monomers are neuroprotective. *J. Neurosci*. 2009, 29, 10582-7.

90) M.L. Giuffrida, F. Caraci, P. De Bona, G. Pappalardo, F. Nicoletti, E. Rizzarelli, A. Copani, The monomer state of beta-amyloid: where the Alzheimer's disease protein meets physiology, *Rev. Neurosci.* 2010, 21, 83-93.

91) I. Benilova, E. Karran, B. De Strooper, *Nature Neuroscience*, 2012, 13, 349-357.

92) I. Autiero, M. Saviano, E. Langella, *Molecular Biosystem*, 2013, 9, 2118-2124.

93) I. Autiero, E. Langella, M. Saviano, *Molecular Biosystem*, 2013, 9, 2835-2841.

94) M.R.H. Krebs, E.H.C. Bromeley, A.M. Donald, *J. Struct. Biol*. 2005, 149, 30-37.

95) P.M. Gorman, C.M. Yip, P.E. Fraser, A. Chakrabartty, Alternate aggregation pathways of the Alzheimer beta-amyloid peptide: Abeta association kinetics at endosomal pH, *J Mol Biol.* 2003, 24, 325, 4, 743-757.

96) Z. Fu, D. Aucoin, M. Ahmed, M. Ziliox, W.E. Van Nostrand, S.O. Smith, *Biochemistry*, 2014, 53, 50, 7893-903.

97) L.M. Young, R.A. Mahood, J.C. Saunders, L.H. Tu, D.P. Raleigh, S.E. Radford, A.E. Ashcroft, *Analyst*, 2015, 140, 20, 6990-6999.

98) S. Sarkar, J.E. Davies, Z. Huang, A. Tunnacliffe, D.C. Rubinsztein, *J. Biol. Chem.* 2007, 282, 5641-5652.

99) P. Spilman, N. Podlutskaya, M.J. Hart, J. Debnath, O. Gorostiza, D. Bredesen, A. Richardson, R. Strong, V. Galvan, *PLoS One*, 2010, 5, e9979.